Study on Evaluation of Traffic Management Measures Using Macroscopic Fundamental Diagram under Flooding Situation

(Macroscopic Fundamental Diagram を用いた洪水発生時の交通管理の在り方の評価に関する研究)

January 2021

Transportation Systems Engineering Major
Graduate School of Science and Technology
Doctoral Course
Nihon University

SUWANNO PIYAPONG

Study on Evaluation of Traffic Management Measures Using Macroscopic Fundamental Diagram (MFD) under Flooding Situation

by

SUWANNO PIYAPONG

A dissertation submitted in partial fulfillment of the requirements for
the degree of Doctor of Engineering

Examination Committee: Professor Dr. Atsushi Fukuda (Chairman)
Nihon University, Japan

Professor Dr. Satoru Kobayakawa
Nihon University, Japan

Professor Dr. Sumio Shimokawa
Nihon University, Japan

Transportation Systems Engineering Major
Graduate School of Science and Technology
Nihon University
Japan

January 2021

ACKNOWLEDGEMENTS

This dissertation could not have been completed successfully without a scholarship from Rajamangala University of Technology Srivijaya and the many suggestions and incredible support offered from numerous people. I would like to thank and dedicate a part of my success to all of them.

First, I would like to express my profound gratitude to my supervisor Prof. Dr. Atsushi Fukuda, for his valuable advice and encouragement throughout my studies at Nihon University. I deeply appreciate his enduring supervision, kindly guidance, unlimited support, and the incredibly valuable time and effort he provided which contributed to my accomplishment. His guidance and recommendations will continue to be crucial in my future professional life.

Second, I would like to express my sincere gratitude to my examination committee members, Prof. Dr. Satoru Kobayakawa and Prof. Dr. Sumio Shimokawa, for their valuable comments and recommendations. I also would like to extend my appreciation to other faculty members of the Department of Transportation Systems Engineering for their valuable comments during my defense preparation. Their suggestions are highly appreciated.

I also would like to use this opportunity to thank Dr. Tuenjai Fukuda for the invaluable guidance given regarding studying a Ph.D. and Assoc. Prof. Dr. Tetsuhiro Ishizaka for supporting me with anything I required when I was new to Doctoral studies.

I would also like to convey special thanks to all the members of the Transportation System Laboratory, especially Dr.Sathita, Mr.Kikuchi, Mr.Higashiyama, Mr.Tsumita, Mr.Roy, Mr.Menegishi, Mr.Ryohei, Mr.Ozawa, Mr.Naoi, Mr.Kouya, Mr.Bob, Ms.Lisako, Ms.Kawaguchi, Mr.Aditya, Mr.Rizky, Mr.Duan, Mr.Asif, Mr.Takano and everyone else for their incessant support in various matters during my stay at Nihon University.

Last but not least, I am highly grateful to Assoc. Prof Dr. Paramet Luathep, my ex-advisor and who has been a great idol in my life, encouraged me each time I was discouraged, and gave me the strength to fight for success.

Finally, I would like to express my deepest appreciation to my beloved parents. I would not have come this far without their constant support and concern. I am forever indebted to them. This dissertation is dedicated to them.

ABSTRACT

Climate change as a result of global warming has precipitated an increase in extreme weather events, with heavy rainfall causing flooding and severe damage in many areas. Asian cities are rapidly becoming more urbanized, and drainage facilities have not been sufficiently developed in low-lying areas where flooding now frequently occurs. Bangkok, the capital city of Thailand, is prone to flooding after heavy rain, with many road sections cut off, causing severe traffic congestion and greatly impacting urban activities. Dealing with this problem requires an accurate understanding of the impacts of floods on road traffic conditions for optimal vehicle management. Many studies have been conducted on hydraulic control measures in Bangkok, but few have examined how to optimize traffic management under flood conditions.

To resolve the problems caused by flooding requires a comprehensive understanding of the extent of flood damage and traffic congestion in specific areas of the city. Here, we propose a method to better understand the impact of urban flood situations by expressing traffic conditions in specific ranges using the concept of a Macroscopic Fundamental Diagram (MFD). The shape of the MFD changes, depending on traffic conditions in a specific range and various flood situations. Through using MFD-based judgment, a road manager can quickly and accurately understand the current traffic situation and take the appropriate traffic control measures. MFD analysis identified traffic flow density and density-velocity relationships by using the shape of the estimated MFD travel time series plots and applies them to the Dynamic Traffic Assignment (DTA) model as traffic flow parameters to suggest a measuring method for road network performance.

The developed model improved road network traffic flow performance under different flood conditions. Finally, a method was presented for evaluating traffic management on the assumption that flooding will occur.

This paper comprises eight chapters, with the contents of each briefly described as follows.

In Chapter 1, the background and purpose of the paper are described, followed by a comprehensive literature review in Chapter 2. The effects of flood occurrence on traffic conditions are assessed using both domestic and foreign literature. Many studies have shown that floods have a severe impact on urban traffic conditions; however, few have detailed how to manage traffic response to floods. Most studies on traffic management measures respond to dynamically changing traffic conditions, and in recent years new

methods for dynamic analysis have appeared using mesoscopic or microscopic traffic simulations. To comprehensively grasp traffic situations using these methods requires analysis of parameters such as free speed and maximum capacity, with macroscopic fundamental design (MFD) as an effective option.

Chapter 3 analyzes the extent of the flooding in Bangkok. Existing studies and various statistical data are organized to clarify the problems caused by floods. Bangkok is located in a lowland area and mechanisms by which inundation height rapidly increases during heavy rainfall due to insufficient drainage systems are explained. Flooding in the city is presented as a distribution map of observed rainfall information, and the relationships between long-term rainfall data and flood occurrence points are analyzed for the Sukhumvit area. Remarkably, the inundation depth suddenly increases even with a small amount of rainfall, causing the closure of many road sections, with serious impacts on traffic conditions.

Chapter 4 estimates traffic conditions based on MFD. Existing studies on MFD are classified, and the MFD concept of parameter estimation is explained. Taxi probe data were collected over one year (2019) in Bangkok to create a time-distance diagram. The slope of the diagram was analyzed, the MFD was drawn, and parameters were estimated in the study area under normal and flooding situations. The inundation depth was further divided into 5 cm units and an MFD was drawn for each flood condition to assess traffic density flow rate and density-velocity regression. Finally, these are clarified to determine traffic flow parameters for free flow velocity, maximum flow rate, and jam density under normal and four different flood conditions.

Development of the mesoscopic traffic model in Chapter 5 evaluates dynamic traffic management under flood conditions. Detailed traffic conditions are analyzed using the mesoscopic traffic model. Model application, use and development are explained. To assess the overall traffic demand, the origin-destination (OD) table obtained by the macroscopic traffic demand forecast was coordinated to match the observed traffic volume, and then the traffic demand in the study area was cut out. We created an OD table for each time interval (15 min) divided into departure time. Next, the mesoscopic traffic model was developed to simulate the traffic conditions of the entire study area. Simulation of the created time zone OD table to the mesoscopic traffic model was performed, and the time zone was adjusted to verify the model based on the observed traffic volume and velocity.

In Chapter 6, the impact of flooding on traffic condition scenarios was analyzed. Different flood conditions and fluctuations in traffic demand were created, and different scenarios were performed using the developed mesoscopic traffic model. The result of each

scenario was compared with the normal situation to evaluate the changes in road network performance in the study area. Firstly, a simulation was performed based on the traffic parameters expressed in the MFD. Indicators of Vehicle Kilometers Traveled (VKT), and Vehicle Hours Traveled (VHT) were adopted as criteria for evaluation of road network performance under normal and flooding situations during peak periods. We calculated the elasticity of the two indicators under different traffic situations. Vehicle Kilometers Traveled was the network usage rate, Vehicle Hours Traveled was the network efficiency, and Vehicle Hours Delay was the service level for each vehicle. Final model performance was evaluated using convergences and link traffic volumes as indicators.

In Chapter 7, traffic management measures in the study area were examined during flooding. Optimized signal system management and traffic demand on arterial roads were induced onto the expressways, and road link performance in the study area was evaluated. Traffic management measures were compared by simulating the developed mesoscopic traffic model to evaluate road link performances. Signal system optimization was assessed using microscopic traffic simulation, with a genetic algorithm based on traffic volume. The optimized signal control system was applied to the mesoscopic traffic model to show the impacts of traffic management measures. As a countermeasure, to reduce the demand of arterial roads, traffic was redirected to the expressway. Implementation of these traffic management measures improved road network performance and traffic flow under flood situations in the study area.

The conclusion as Chapter 8 summarizes the results and future prospects. This paper focused on the impact of frequent floods, especially in Asian cities, on traffic conditions and analyzed the traffic using taxi probe data in the study area under both normal and flooding conditions. We drew the MFD and estimated traffic flow parameters to show the impacts on traffic under normal and flooding situations. The obtained parameters were applied to the mesoscopic traffic model to simulate scenarios that combined different flooding situations and variation of traffic demand. The impacts of traffic management measures were clarified for effectiveness. The taxi probe data used in this study has proved effective in many cities as a highly feasible method.

TABLE OF CONTENTS

LIST OF TABLES

LIST OF FIGURES

CHAPTER 1

INTRODUCTION

1.1 Background

Global climate change has induced extremes of rainfall in terms of frequency, duration, pattern, and intensity in many cities of developing countries. The percentage of extreme rainfall compared to the total has also significantly increased, with a further increase of 9.65% forecast from 2011 to 2099 [1]. Intense rainfall has been recorded in many developing cities undergoing rapid urbanization such as Bangkok in Thailand.

The process of urbanization unfolds following complex mechanisms. Rapid urbanization inevitably results in underdeveloped drainage systems that have inadequate maintenance [2]. Figure 1.1 shows development plan sequences of urban Bangkok from 1907 to 1997.

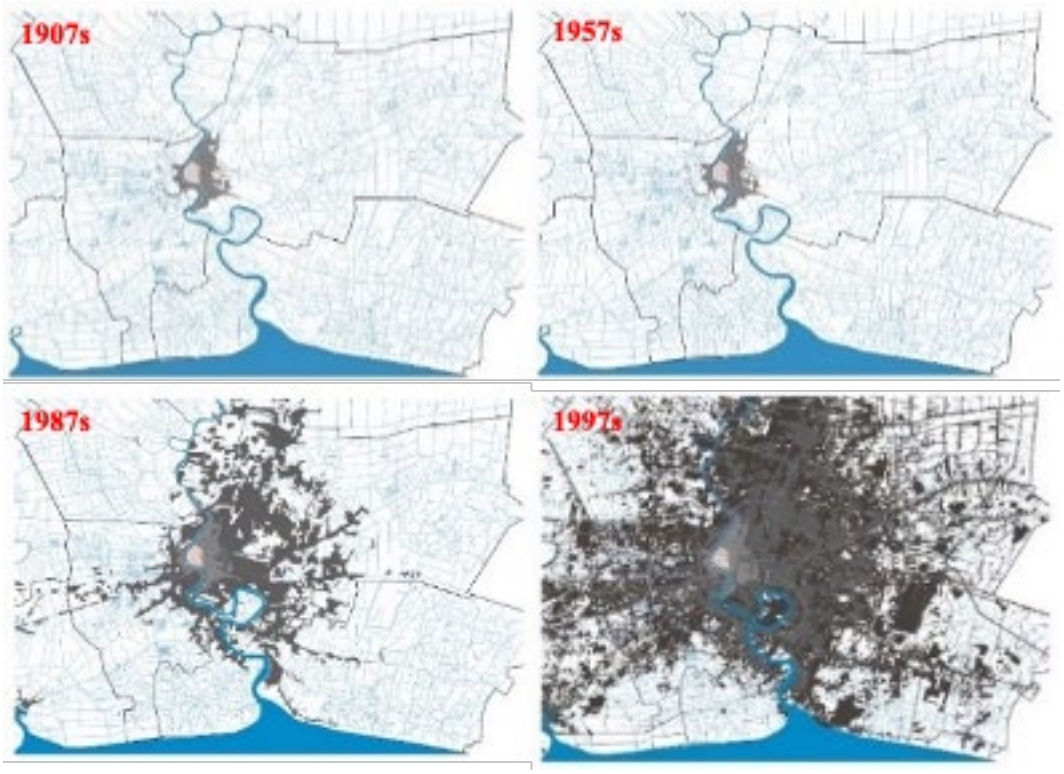

Source: Urban Design and Development Center

Figure 1.1 Expansion of the urban Bangkok

Under such a scenario of rapid urbanization, excessive rainfall results in road floods that negatively impact everyday human decisions and activities. Drivers have to modify their travel patterns by taking different routes, leaving for destinations at different times, or canceling the trip altogether. To better understand and minimize the traffic impact of different flood conditions, flood-related data must be integrated with road usage statistics.

Flood conditions that reduce the average driving speed on an arterial road can be mitigated by quickly implementing traffic signals to lower speeds while still maintaining orderly progression through the network. However, development and implementation of strategies that minimize the effects of adverse flood conditions require comprehensive knowledge of how flood events impact traffic operations, and how best to assess the flood-related effects for a given scenario.

Previous research integrated flood simulation with traffic analysis to model different viewpoints of the interplay between these two spatiotemporal phenomena. This integration allows building a road network model to assign trip paths, consider the effects of road closures, and evaluate travel delays and vehicle volume redistribution in a given flash flood scenario [3] by considering the influence of floods on mobility, mainly focusing on severe flood conditions. The relationship between flood events and traffic operations was assessed by a microscopic traffic simulation model that could handle complex roadway geometrics, traffic control devices, and vehicle configurations.

However, if the key parameters within a microsimulation model could be changed under various flood conditions, this would greatly assist in developing improved flood-responsive traffic management strategies.

Traffic flow theory studies the interactions between travelers and infrastructure and can be used to rationally explain changes in traffic phenomena under different road network conditions. The concept of Macroscopic Fundamental Diagram (MFD) was first proposed by Greenshields [4] to establish a relationship between volume, speed, and density. MFDs are used to understand and comprehend traffic flow characteristics in complex urban networks [5, 6] and also to evaluate the performance of traffic control strategies. The number of MFDs indicates the existence of different levels of service on different network routes. The shape of the MFD generally depends on network topology, traffic flow, rate of incoming traffic, peak/off-peak period, vehicle route choice, signal timing plans at the intersections, and infrastructure characteristics [7, 8].

Previous studies on MFD estimation relied on fixed loop detector data. However, the cost of installation and operation of roadside loop detectors is often high and, therefore, detectors cannot economically be used everywhere. In developing countries, traffic detectors are usually concentrated on arterial roads and highways. With recent advances in GPS-enabled devices, mobile probe vehicles can now provide information on location, speed, and distance traveled at regular intervals within a road network. Probe vehicles offer remarkable advantages compared with conventional static detectors.

Here, the impacts of flood conditions on traffic operations in an urban network were assessed by analyzing changes in the key parameters of MFD using probe vehicle trajectories during flood days. MFD parameters can be used to estimate the relationship between free-flow speed, maximum flow, and traffic jam density for road surfaces under varying flood depths. Results can then be used to build a road network model to determine optimal travel routes by considering the effects of road degradation to assess travel delays and vehicle distribution in a given road flood.

1.2 Statement of Problem

Previous studies identified that rain intensity impacted MFD shape as a weak correlation factor since rainfall measurement alone does not take into account flow paths of fast-running water and areas where the water pools deeply to block roads completely. An accurate assessment of the impacts of different flood conditions on MFD shape has not been previously undertaken in large road networks.

Development of empirical relationships between depth of flood water and vehicle speed reduction cannot analyze impacts at network macroscale that require relevant parameters of speed, flow, and density. To resolve this problem, this study assesses how MFD parameters change with flood conditions and applies the results to generate a traffic model to analyze the impacts on a whole network.

1.3 Purpose and Objectives

The aim of this dissertation is to study on Evaluation of Traffic Management Measures Using Macroscopic Fundamental Diagram under Flooding Situation in urban Bangkok, Thailand. The specific objectives are as follows.

- Understand and comprehend the MFD shape under different flood depths to gain a more profound knowledge of MFD dynamics and properties.
- Develop and validate traffic modeling for the urban Bangkok road network.
- Apply MFD to the Bangkok road network and compare the results of different flood parameters.

1.4 Scope of Study

The research scope was divided into two main sections as the study area and the baseline model.

First, the study area considered the availability of information to achieve objective 1; namely traffic data (probe data), flood data (historical data), and other relevant information. Sukhumvit occupies the eastern part of the commercial district of Bangkok. This area was selected for study due to the frequent occurrence of flooding. In Sukhumvit, even light rains can cause road floods and consider flood depth not exceeded 30 cm [9].

Second, the baseline model as the static model was improved from the model currently in use in Thailand. Then the improved baseline model was imported into a dynamic model to evaluated road networks and travel information, including demand forecasting for future projects as described in Chapter 5, and focused on an average weekday morning peak period for road passenger traffic. The main study interest concerned the performance of the transport system when placed under extreme pressure.

1.5 Dissertation Outline

This dissertation consists of seven chapters as shown in Figure 1.2.

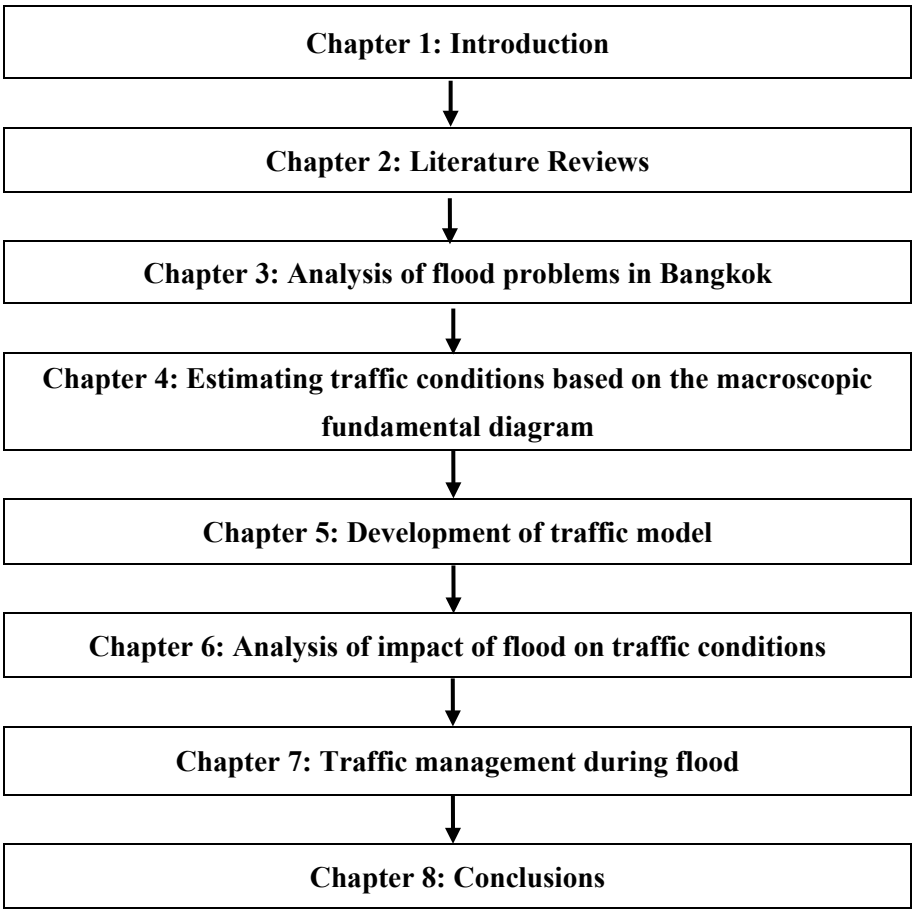

Figure 1.2 Structure of dissertation

REFERENCES

1. Masud, M.B., et al., Changes in climate extremes over North Thailand, 1960–2099. Journal of Climatology, 2016.

2. Shepherd, J.M. and S.J. Burian, Detection of Urban-Induced Rainfall Anomalies in a Major Coastal City. Earth Interactions, 2003. 7(4): p. 1-17.

3. Hu, S., et al. Impacts of Rain and Waterlogging on Traffic Speed and Volume on Urban Roads. in 2018 21st International Conference on Intelligent Transportation Systems (ITSC). 2018. IEEE.

4. Greenshields, B.D., A study in highway capacity. Highway Research Board Proc., 1935, 1935: p. 448-477.

5. Geroliminis, N. and C.F. Daganzo. Macroscopic modeling of traffic in cities. in Transportation Research Board 86th Annual Meeting. 2007. No. 07-0413.

6. Geroliminis, N.D., Carlos F, Existence of urban-scale macroscopic fundamental diagrams: Some experimental findings. Transportation Research Part B: Methodological, 2008. 42(9): p. 759-770.

7. Geroliminis, N. and J. Sun, Properties of a well-defined macroscopic fundamental diagram for urban traffic. Transportation Research Part B: Methodological, 2011. 45(3): p. 605-617.

8. Geroliminis, N. and B. Boyacı, The effect of variability of urban systems characteristics in the network capacity. Transportation Research Part B: Methodological, 2012. 46(10): p. 1607-1623.

9. Hilly, G., et al., Methodological Framework for Analysing Cascading Effects from Flood Events: The Case of Sukhumvit Area, Bangkok, Thailand. Water, 2018. 10(1): p. 81.

CHAPTER 2

LITERATURE REVIEW

This chapter reviews many studies on how flood occurrence impacts traffic conditions. These reports introduce the basic characteristics of an MFD and estimate how traffic in urban networks affects MFD shape. The principles of dynamic traffic modeling are also reviewed.

2.1 Effects of flood occurrence on traffic conditions

Road transportation plays an important role in day to day life. However, efficiency is impacted by many aspects including climate change. Flooding causes excessive delays in the road transportation network. The vulnerability of transportation networks has attracted increasing attention and a comprehensive understanding of the root causes of delays can enhance prevention and response capabilities during disaster events and emergency incidents.

A plethora of research concerned with transportation network vulnerability has proposed different solutions from diverse approaches. However, no strong consensus exists on the definition of transportation network vulnerability and the optimal evaluation methodology. This comprehensive literature review provides a clear understanding of previous methods as a good basis for developing improved procedures. The current literature presents several methodologies for addressing transportation network vulnerability.

Chen et al. [1] analyzed transportation network vulnerability using new accessibility-based methodology to evaluate travel modes under flooding impacts in Hillsborough County, Florida. They verified the established model using ArcGIS to identify the inundated segments. Different flooding scenarios were applied in CUBE to update the shortest travel time changes under flooding. Networkwide accessibility and vulnerability values under each scenario were then calculated. Finally, accessibility values calculated with the proposed accessibility-based method and the Hansen accessibility index method were compared. Results for the two methods were similar. The proposed method yielded normalized values that made the results clearer and provided increased levels of accessibility loss. Their results supported decision-making for urban transportation under flooding disasters resulting from extreme weather events and sea level rise.

Stamos et al. [2] studied the impacts of extreme weather events and natural disasters on transportation systems in 13 European cities. They developed a modal split model comparing the percentage change of passenger trips between different modes and evaluated the vulnerability of transportation networks after modal split changes. However, modal split results of the binary logit model were not validated with field observation data under extreme weather events, while factors influencing the mode choice for different nations or regions were not considered in the modeling process.

Cools at al. [3] focused on the effect of weather conditions on daily traffic intensities in Belgium to determine whether road usage in a particular location determined the size of the impacts of various weather conditions. They analyzed the effects of weather conditions on both upstream (toward a specific location) and downstream (away from a specific location) traffic intensities at three traffic count locations typified by different road usages. Their results indicated heterogeneous weather effects between different traffic count locations on upstream and downstream traffic. Snowfall, rainfall, and wind speed also diminished traffic intensity, while high temperatures increased traffic volume.

Stern et al. [4] examined weather impacts on 33 road segments in metropolitan Washington, D.C. from December 1999 to May 2001. Eighteen of the segments were freeways and 15 roads were major arterials (covering 239 miles). Reported travel time and weather observation data were combined and utilized in a two-step regression analysis to predict travel time impacts under adverse road weather conditions. Initially, travel times were regressed against selected weather variables. In the second step, linear regression models for each road segment were reduced and used to predict normal travel time as well as increased travel time due to weather. Weather variables included precipitation (none, light rain/snow, heavy rain, or heavy snow/sleet), wind speed (<30 mph or ≥ 30 mph), visibility distance (≥ 0.25 miles or <0.25 miles), and slick pavement conditions (dry, wet, snowy, or icy).

Hilly et al. [5] described a methodological framework to analyze the cascading effects from floods that was applied to the Sukhumvit area of Bangkok. Results suggested that the effects from floods were much broader in their reach and magnitude than the sole impacts incurred from direct and immediate losses. In Sukhumvit, these included loss of critical services, assets and goods, traffic congestion and delays in transportation, loss of business and income, disturbances and discomfort to the residents. All these losses were analyzed in detail as cascading effects. Different visualization options including a casual loop diagram, a HAZUR resilience map, a tree diagram and GIS maps were employed to display the findings.

2.2 Application of a Dynamic Traffic Assignment

2.2.1 Introduction

Traffic can be categorized into static and dynamic assignment models. Static traffic assignment (STA) assumes that link flows and link travel times remain constant over the modeling horizon, while in dynamic traffic assignment (DTA) models the link flows and link travel times are time-variant. DTA has become an increasingly popular tool to assess the performance of traffic infrastructure and analyze the behavior of drivers. STA cannot consider the effects of variations in traffic flows over time, dynamic changes in transportation systems, congestion impacts, and advanced strategies and technologies. With the implementation of dynamic user equilibrium and the time-dependent nature of demand and network characteristics, a DTA model produces more realistic traffic conditions on a large scale. DTA model analysis results can be used to evaluate many meaningful measures related to individual travel time and cost, as well as systemwide network measures for regional planning purposes. The main assignment components are shown in Table 2.1.

A DTA published by the Transportation Research Board (TRB) addressed the core concepts necessary for understanding DTA in relation to static traffic assignment (STA) in terms of “equilibrium” [6] relevant to system optima of Wardrop’s principle [7]. This is typically based on the premise that the experienced travel time for all used routes is the same for travelers departing at the same time. Many models and algorithms have been developed in the domain of equilibrium-based DTA since the 1970s [8-12].

Table 2.1 Comparing Static and dynamic Assignment models

Features	Static Traffic Assignment	Dynamic traffic Assignment
Demand	Fixed for a given time period (peak hour)	Variable, reflecting the profile of variation by slices
Network link attributes	Fixed for a representative1-hour period (capacity, volume, etc.)	Some attributes like capacity may be fixed, but demand and performance vary dynamically for each time interval
Network (intersection details)	Intersection delays are not explicitly modelled	Delays at intersections modelled using signal timing
Arterial links with signalized intersections	Traffic flow on a link is unconstrained No "blocking back" or "queue spill back"	Link flows represent "actual demand" impeded by capacity at junctions
Predictors	Volume-delay functions -Free flow speed (km/hr.) -Lanes -Capacity per lane (veh/hr.) -Alpha & beta coefficients	Flow density relationships -Free flow speed -Effective length factor -Response time factor
Output	Link travel time (min)	Maximum flow (vol/h/lane) Jam density (vol/km/lane)
Other	Inflow=Outflow No link spillback VC ratios – correlate to congestion through "average" level-of-service First-In-First-Out Representation of links – no individual lanes Unable to represent interaction of traffic with signalized intersections	Inflow ≠ Outflow Link spillback can happen Flow dynamics ensure direct linkage between travel time and congestion Vehicles can overtake other vehicles /vehicles can have different travel times & speeds Individual lanes / Independent traffic conditions of separate lanes Able to model interaction of traffic with signalized and un-signalized intersections

2.2.2 Dynamic equilibrium solution algorithm

The solution algorithm used here consists of two main components: 1) a method to determine a new set of time-dependent path flows given the experienced path travel times on the previous iteration, and 2) a method to determine the actual travel times that result from a given set of path flow rates. The latter problem is referred to as the ''network-loading problem" and can be solved using any route-based dynamic traffic model. The algorithm requires a set of initial path flows, which are determined by assigning all vehicles to the shortest paths, based on free-flow conditions. The general structure of the algorithm is shown schematically in Figure 2.1.

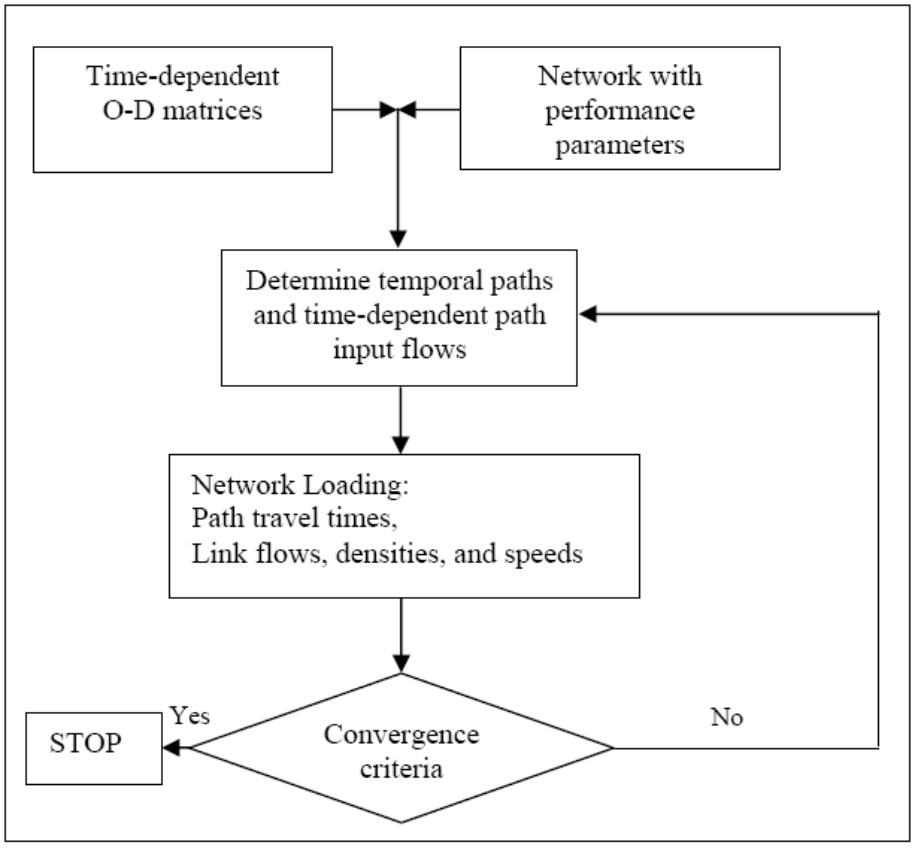

Figure 2.1 Structure of the solution algorithm for the Dynamic model

The mathematical statement of the dynamic equilibrium problem was summarized by Mahut [13] who referenced research of [14-17]. The demand is subdivided into discrete time periods called departure intervals (τ). Each τ has the demand (g_i^τ) for each O-D pair ($i, i \in I$). The initialization procedure consists of an incremental loading scheme that successively assigns the partial demand for each interval τ onto dynamic shortest paths. In successive iterations, the path input flows (h_i^τ) for each path ($k \in K$) are determined by the method of successive averages (MSA) applied to each O-D pair *i* and departure interval τ.

Starting at the second iteration, the time-dependent link travel times obtained by the network loading model are used to compute new path travel times s_i^τ, for each path k and each departure interval τ (i.e., for used and unused paths).

The travel time on the shortest path for O-D pair i and departure interval τ is denoted h_i^τ. For each iteration l, up to a pre-specified number of paths per O-D pair, *N*, the set of new shortest paths is added to the current set of paths. The volume assigned as the input flow to each path is $g_i^\tau / l,\ i \in I$, all τ.

For $l > N$, only the shortest among used paths is identified: no new paths are added, and the path input flow rates are redistributed. The algorithm may be stated as follows.

	Dynamic MSA Equilibration Algorithm
Step 0	$l = 1$; compute dynamic shortest paths based on free-flow travel times, and load the demands to obtain an initial solution; $l = l + 1$;
Step 1	If $l \leq N$, compute a new dynamic shortest path and assign to each path $k \in K$ the input flow g_i^τ / l If $l > N$, identify the shortest among used paths and redistribute the flows as follows:

$$h_i^{\tau(l)} = h_i^{\tau(l-1)}\left(\frac{l-1}{l}\right) + \frac{g_i^\tau}{l} \quad if \quad s_k^{\tau(l-1)} = u_i^{\tau(l-1)}$$

$$h_i^{\tau(l)} = h_i^{\tau(l-1)}\left(\frac{l-1}{l}\right) \qquad otherwise \tag{2.1}$$

$$for \quad k \in K, \qquad i \in I \quad and \quad all \quad \tau$$

Step 3	If l is less than a pre-specified maximum number of iterations, or $RGap \leq \varepsilon$, Stop; otherwise return to step 1

A measure of the gap (as used in static network equilibrium models) can be used for qualifying a given solution. This is the difference between the total travel time experienced and the total travel time that would have been experienced if all vehicles had the travel time (over each interval τ) equal to that of the current shortest path.

$$RGap^{\tau(l)} = \frac{\sum_{i\in I}\sum_{k\in K} h_i^{\tau(l)} s_i^{\tau(l)} - \sum_{i\in I} g_i^\tau u_i^{\tau(l)}}{\sum_{i\in I} g_i^\tau u_i^{\tau(l)}} \tag{2.2}$$

The relative gap measure is used in DTA to indicate how close an assignment is to dynamic user equilibrium (DUE). DUE is achieved when, for a given departure time interval, all used paths connecting an OD pair have the same travel time. No user can improve their travel time by switching paths, and this is true for all OD pairs. A relative gap of zero would thus indicate a perfect dynamic user equilibrium flow.

2.2.3 Description of mesoscopic model

A brief overview of the mesoscopic model is given based on the user manual. Mesoscopic is an equilibrium-based model that iterates between finding time-dependent path flows and determining the corresponding path travel times. Vehicles are assigned to paths using the Method of Successive Averages (MSA), which assigns a decreasing fraction of vehicles to the shortest path in subsequent iterations. The fraction is equal to one divided by the current iteration number. Thus, in the first iteration, all vehicles are assigned to the shortest path, while half of all vehicles are assigned to the shortest path in the second iteration. Vehicles are simulated at a microscopic level to determine path costs.

The three components of traffic flow are car following, gap acceptance, and lane changing. These represent the interactions between vehicles that lead to traffic congestion.

1) The mesoscopic traffic simulation uses a simplified car-following model that is expressed as follows:

$$x_f(t) = MIN[\left(x_f(t-R) + V_{free} \times R\right), (x_l(t-R) - L] \tag{2.3}$$

Where $x_f(t)$ = position of the following vehicle at time *t*
$x_l(t)$ = position of the leading vehicle at time *t*
V_{free} = free speed of the roadway
L = effective length of following vehicle,
R = response time of following vehicle.

Car-following models also describe the steady-state properties of traffic on a roadway. Steady-state properties are those that can be observed when the traffic is moving at a constant speed, and thus also at a constant flow and density. The relationship between the steady-state values of speed, flow, and density is called the fundamental diagram of traffic. This shows the three macroscopic traffic flow parameters as maximum flow, jam density and wave speed.

For mesoscopic, a triangular shaped diagram was chosen. This can be described by only three parameters, thereby minimizing the required input data. The triangular shaped diagram is presented below.

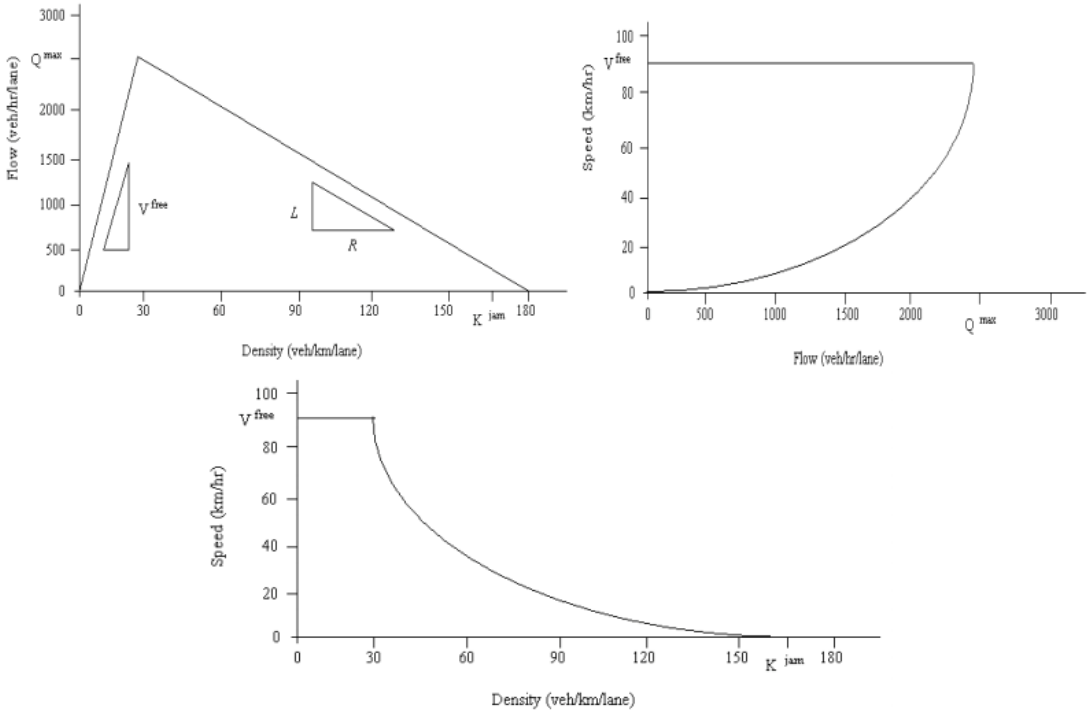

Figure 2.2 The basic relationship of traffic flow of car-following in mesoscopic

The diagrams show the following three macroscopic traffic flow parameters:

- Maximum flow (Qmax) is the maximum possible flow rate (expressed in veh/hr, or veh/hr/lane) that a specific link can carry of a specific vehicle type.

- Jam density (Kjam) is the maximum number of vehicles of a specific vehicle type (expressed in veh/km or veh/km/lane) that fit on the roadway when standing still.

- Wave speed (Vwave) is the speed (km/hr) at which shock waves move through a platoon of traffic against the direction of flow, for a specific vehicle type. When a traffic signal turns green, the time between when the first and last vehicles standing still in line begin to move, divided by the distance between them, is equal to the wave speed.

Values of the three macroscopic traffic flow parameters for a specific vehicle type and a specific roadway can be determined from the free speed of the link, the effective length (L), and response time (R) of the vehicle type as follows:

$$Q_{max} = \frac{1}{(R+\frac{L}{V_{free}})} \tag{2.4}$$

$$K_{jam} = \frac{1}{L} \tag{2.5}$$

$$v_{wave} = \frac{L}{R} \tag{2.6}$$

The flow vs. density diagram, which shows all three of these parameters, can be interpreted as follows. The level of congestion is represented by density, which increases on the horizontal axis from zero to the jam density. On the left side of the diagram, the value of flow increases with density until reaching the maximum flow. This line describes the steady-state behavior of traffic in nonconnected conditions. On the right side of the diagram, the flow decreases with increasing density until reaching a value of zero at the jam density. At this point, traffic is standing still. This line describes the steady-state behavior of traffic in congested conditions. The steady-state speed of the traffic at any point on this diagram is the slope of the line from the origin of the graph to that point. Thus, speed remains constant and equal to the free speed in nonconcerted conditions. In congested conditions, speed decreases with increasing density, and is equal to zero at the jam density.

2) A gap-acceptance stochastic model determines whether a vehicle on a lower priority movement precedes a vehicle on a conflicting higher-priority movement. Gap acceptance is modeled in Mesoscopic based on two quantities as the available gap and the relative wait. The available gap is the amount of time available for the lower priority vehicle to execute its movement and clear the point of conflict with the higher priority vehicle. The relative wait is the difference between the amount of delay that two vehicles have already incurred at an intersection (not including delay due to a red traffic signal) as the next vehicles to exit by their respective lanes. This delay is the amount of time spent waiting for acceptable gaps in higher-priority movements. More detailed information can be found in the Mesoscopic user manual.

3) Lane changing, Mesoscopic models the movement of vehicles on individual lanes of a roadway. How drivers utilize the lanes on the road can have a significant impact on delays and how these delays propagate through the network. Since vehicle trajectories within links are modeled implicitly, each driver must choose the lane by which to exit a link just before entering it. Once on the link, the choice is not re-considered. The rules used to model drivers' lane-choice behaviors are complex, combining a look-ahead procedure with local lane-choice rules. The look-ahead feature captures the behavior of drivers familiar with the roadway and the recurrent congestion patterns along their usual paths.

2.3 Basic idea of the macroscopic fundamental diagram

Traffic flow is the study of interactions between travelers and infrastructure, with the aim of understanding and developing an optimal transport network, with efficient movement of traffic and minimal traffic congestion problems. Traffic flow theory on the fundamental diagram (FD) [18] shows the relation between flow, density and speed. The macroscopic fundamental diagram (MFD) is a relatively new generalization of FD basic that relates space-mean flow ($\bar{q}$), density ($\bar{k}$), and speed ($\bar{v}$) of an entire network with n number of links, as shown in Figure 2.3.

The MFD thus represents the capacity $\mu(\eta)$ of the network in terms of vehicle density, with μ being the maximum capacity of the network and being the jam density (η) of the network. The maximum capacity or "sweet spot" of the network is the region at the peak of the MFD function.

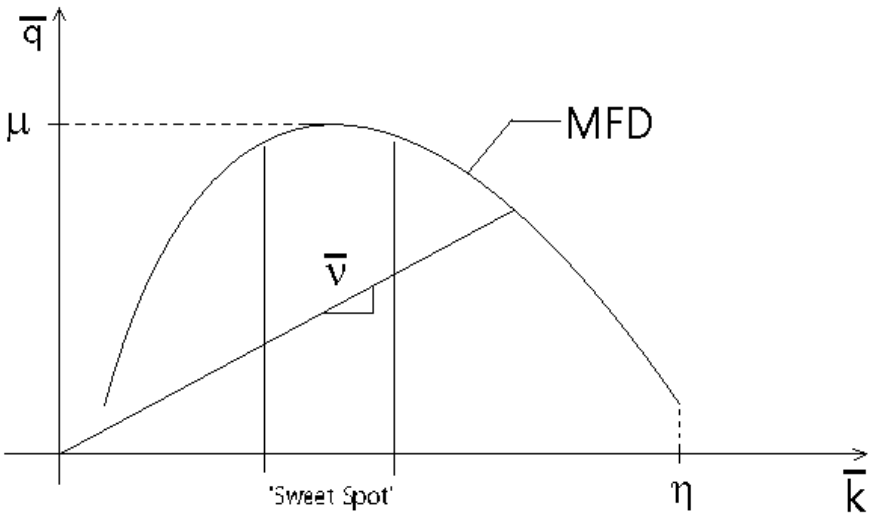

Figure 2.3 Sample traffic flow macroscopic fundamental diagram

The MFD concept was first introduced by Godfrey [19] who found a parabolic relationship between the average travel speed and vehicle kilometers traveled on the Central London road network, with speed determined as inversely proportional to traffic density. In 2007, Daganzo [20] proposed a solution to decrease congestion by developing an adaptive perimeter control mechanism that used the MFD concept to monitor and control the number of vehicles entering a neighborhood. This adaptive control approach developed the modeling of urban gridlock phenomena for single neighborhoods and for systems of interconnected neighborhoods with macroscopic variables, under vehicles leaving and accumulating in the system.

However, this model of large-scale arterial networks was not realistic and appropriate to deal with crowded conditions. Geroliminis et al. [21] introduced macroscopic control strategies in downtown San Francisco and presented a diagram of production (flow) and accumulation (density) of vehicles. They used Edie's definitions [22] to estimate mean flow and mean. Results showed MFDs as curves that can be reproduced under homogeneous conditions in urban networks.

Empirical verification of the MFD existence of Geroliminis and Daganzo [23] through the combination of measurements from 500 fixed detectors in Yokohama City of Japan. These detectors did not cover the entire network, so GPS taxi data was used with full network coverage to produce the flow-occupancy relationship. Results showed that the flow and occupancy relationship produced by data from fixed detectors contained a large amount of scattering, while proximity fixed detectors did not represent the whole network. Data from GPS-equipped taxis produced a smoothly declining curve with deviations smaller than those obtained using fixed detectors. The analysis also revealed a fixed relation between space-mean flows on the whole network, which can be used to estimate MFD on neighborhood-sized sections of cities independently of the demand. This can also be used to control demand to improve accessibility by modifying the infrastructure, since the amount of street space allocated to cars and buses, street closures, flyover construction, or new signal timings surely affect a neighborhood's MFD.

2.3.1 Applications

Geroliminis and Daganzo [23]proposed the outflow rate provided by the MFD as a way to evaluate the accessibility of the city and determine how this could be improved by taking certain measures. If a new control strategy is implemented or an infrastructure change occurs, the MFD will most probably change; maximum production will increase or decrease depending on the success of the measure. Evaluation of the measurements can

only take place in the area where the measure was applied, and the effect could be falsely overestimated due to narrow exploration of the results. For example, the implementation of a new traffic control algorithm at one intersection could improve the flow, only because drivers now choose another intersection. This false assessment could have been avoided by examining results in the complete network.

Daganzo [20] proposed a solution to decrease congestion by developing an adaptive perimeter control mechanism that used the MFD to monitor and control the total number of vehicles that entered a neighborhood. The idea was tested by Geroliminis and Daganzo [21]at two simulated sites in Lincoln Avenue, Los Angeles and in downtown San Francisco. They maximized the outflow by maintaining the total number of vehicles inside the network at the optimal level and restricting vehicle entry. Results showed that the perimeter control worked as expected, and outflow increased by 34%. They also proved that outflow and travel production were linearly related.

Keyvan et al [24] also analyzed the application of a perimeter control strategy. They proposed the use of the MFD to apply a "feedback-based gating" as a test application of the gating strategy. The simulation offered encouraging results with fewer delays and higher speeds in the simulated network.

Geroliminis and Levinson [25] utilized the MFD to sketch a network-based congestion pricing scheme. This was tested in the same site used by [23]at Yokohama, Japan for the morning peak rush hour. Their results showed that the toll-case worked very well compared to the no-toll case. When applying the optimal toll price, delays were eliminated, and the duration of the peak hour decreased. Simoni et al. [26] also proposed a methodology to derive time-dependent toll prices using a network fundamental diagram. They tested their methodology in a simulated case study of the city of Zurich. They found that this approach was more realistic than the analytical methods usually applied to decide tolling schemes. Their proposed approach needed only scant information and offered a very good representation of the traffic dynamics.

Instead of applying a limit to the inflow in the network, as proposed by the preceding gating and pricing strategies, the MFD could also be used to implement a routing strategy to spread vehicles over the network. Such a routing strategy was proposed by Knoop et al. [27]. They suggested routing traffic using the MFD in a way that avoided oversaturation. Their results showed an improvement in traffic flow [28] also proposed a "route guidance advisory control system" as an optimal state for the network. Homogeneous conditions play an important role in routing strategies and further research is required on this aspect.

Various studies have investigated the advantages of applying the MFD to support new traffic control strategies or to assess existing strategies. These findings strengthen the allegation that although the MFD is simple and parsimonious, it can be very useful and powerful. The simplicity of the MFD is one of its strongest points and motivates research on the topic.

2.3.2 Data and Methodology

The MFDs produced to date were based either on traffic data from the real world or on simulated data. Instead of using traffic data,[29] and later [30] derived an analytical method to derive an MFD that avoided the necessity of large amounts of data. Their goal was to produce a general model that could be used to acquire the MFD for any network. They acknowledged that networks are affected by multiple and complicated variables and tried to derive an estimation method with as few parameters as possible. Their proposed method produced an upper bound of the average flow in the network that complied with some regularity conditions. Leclercq and Geroliminis [31] further extended and improved this methodology by relaxing some of the regularity conditions. However, the proposed methodology still had disadvantages and required homogeneous congestion levels in the network.

2.3.3 Using real traffic data

Geroliminis and Daganzo [23] were the first to derive a smooth network fundamental diagram from real data, using loop detector data from downtown Yokohama in Japan. The flow-occupancy relationship produced by their data from individual detectors contained a lot of scatter; however, when aggregating the detector data, a smooth relationship was achieved. The detectors did not cover the entire network. They produced the same relationship using GPS taxi-data that had full network coverage and created a relationship between space-mean speed and density. The smooth graph produced indicated that an MFD could exist as a characteristic for the entire urban network [32] used unweighted mean formulas with loop detector data from both highways and surface road networks to create an MFD in Toulouse, France.

They monitored the evolution of flow and occupancy throughout selected days of analysis to determine whether heterogeneity applied in the network. More specifically, they examined the homogeneity issue with regard to different road types, distance of the loop

detectors from the stop line, and congestion levels throughout the network, and investigated how each parameter influenced scatter on the MFD.

Another study used detailed vehicle trajectories from freeway stretches as real data to estimate the MFD [33]. Results showed that an MFD could only be produced if the network was in a congested or uncongested state, not in a mixed state. They also discovered that MFDs for freeways could also be produced by loop detector data. This required at least one detector per link, with the data filtered to meet the single regime condition.

2.3.4 Using traffic simulation data

Geroliminis and Daganzo [21] performed various microsimulations in downtown San Francisco. They were the first to produce a diagram relating production to accumulation of vehicles, with the aim of applying macroscopic feedback control strategies. They used Edie's definitions [22] to estimate mean flow and mean density.

Courbon and Leclercq [34] used a microsimulation model to compare three different ways to produce the MFD. They wanted to avoid the bias resulting from use of empirical data and have complete control over the urban environment and the traffic phenomena occurring within. The three different approaches were 1) Using loop detector data and the weighted averages, as in Geroliminis and Daganzo [23], 2) Using analytical methods with cuts proposed by [29], and 3) Using data from vehicle trajectories. Their very simple network included road sections of similar length and the same traffic light cycle. Results showed that the trajectory method produced the MFD very accurately in all network shapes. They suggested that this method could be used as a baseline to evaluate and compare other methods.

Keyvan et al. [24] used simulation data from the city of Chania, Greece to produce the MFD and test their proposed gating measures to improve mobility. They stated that an MFD can be either "ideal" when it includes the precise traffic data of all network links and can only be derived from simulation environments, or "operational" when it includes the available traffic data from a subset of the network links. An "operational" MFD can be "complete" if the available traffic data cover the entire set of network links. For testing, they produced a "complete operational" MFD. In combination with a moderate number of real-time measurements, this can describe the traffic situation and determine the appropriate gating strategy. They used all measurements of the links to detect the point on the MFD where their network was operating. However, they suggested that this was not

needed, and that the information required for gating could be extracted using less real-time measurements.

2.3.5 Influencing factors

Research on the impact of homogeneity at the shape of the MFD was performed by [33]. They found that homogeneity at network congestion level was necessary to have an MFD. Heterogeneous increase of congestion in space led to hysteresis effects on the MFD. They concluded that "congestion spreading must be homogeneous" [35] supported this allegation using simulation data. They found that when congestion starts and resolves homogeneously, a reduction in flow occurs. They suggested a solution to this problem using ramp metering to create homogeneous traffic states in the network.

Geroliminis and Daganzo [23] separated the signalized and non-signalized roads of Yokohama to derive an MFD without scatter. They did not consider the highways because homogeneous road types were required for an accurate MFD. The same conclusion was drawn by [32] who recommended that the city should be divided into zones, taking into consideration geographic characteristics and road types. Within zones of the same road type, they highlighted the importance of separating signalized and non-signalized roads to avoid scatter in the MFD.

Geroliminis and Sun [36] found that the MFD did not hold for freeway networks due to their different characteristics such as the absence of traffic signals, hysteresis effect and different speed levels. This finding was based on real data from an experiment conducted in Twin Cities, Minnesota. By contrast, Cassidy et al. [34] suggested that the MFD could also be produced in any freeway network if all the links were either in the congested or the uncongested state.

Buisson and Ladier [33] separated the detector data into three categories according to the detector distance from the traffic light. They found that this distance strongly impacted the slope of the MFD. Therefore, they recommended the use of detectors at similar distances from the traffic signal. Courbon and Leclercq [34] discovered that when the loop detectors were equidistant from the traffic signal, results were not representative. They suggested that the detectors should be "spread upstream, and downstream of the traffic signal, and in the middle of the section" so that they covered all the possible traffic states.

Laval and Castrillon [38] investigated the effects of signal timing on the MFD. They focused on the length of the cycle, the ratio of green to red and coordination using both simulated and empirical data from Yokohama, Japan. Their results suggested that two parameters played the most important roles on the shape of the MFD as the mean ratio of the block length to green and the mean ratio of red to green light.

REFERENCES

1. Chen, X.-Z., et al., Analysis of transportation network vulnerability under flooding disasters. *Transportation research record*, 2015. Vol.2532(1), p.37-44.

2. Stamos, I., et al., Impact assessment of extreme weather events on transport networks: A data-driven approach. *Transportation research part D: transport and environment*, 2015. Vol.34, p.168-178.

3. Cools, M., E. Moons, and G. Wets, Assessing the impact of weather on traffic intensity. *Weather, Climate, and Society*, 2010. Vol.2(1), p.60-68.

4. Stern, A.D., et al. Analysis of weather impacts on traffic flow in metropolitan Washington DC. *19th international conference on interactive information and processing systems (IIPS) for meteorology, oceanography, and hydrology*. 2003.

5. Hilly, G., et al., Methodological Framework for Analysing Cascading Effects from Flood Events: The Case of Sukhumvit Area, Bangkok, Thailand. *Water*, 2018. Vol.10(1), p.81.

6. Chiu, Y.-C., et al., Dynamic traffic assignment: A primer. Dynamic Traffic Assignment: *A Primer*, 2011.

7. Wardrop, J.G. and J.I. Whitehead, Correspondence. some theoretical aspects of road traffic research. *Proceedings of the Institution of Civil Engineers*, 1952. Vol.1(5), p. 767-768.

8. Merchant, D.K. and G.L. Nemhauser, A model and an algorithm for the dynamic traffic assignment problems. *Transportation science*, 1978. Vol.12(3), p.183-199.

9. Ghali, M. and M. Smith, Road pricing: a new model for assessing the many options. *Traffic engineering and control*, 1992. Vol.33(3), p.156-157.

10. Mahmassani, H., et al. Dynamic traffic assignment with multiple user classes for real-time ATIS/ATMS applications. *Proceedings of the Advanced Traffic Management Conference Federal Highway Administration*. 1993.

11. Boyce, D., D.-H. Lee, and B. Ran, Analytical models of the dynamic traffic assignment problem. *Networks and Spatial Economics*, 2001. Vol.1(3-4), p.377-390.

12. Florian, M., M. Mahut, and N. Tremblay. A hybrid optimization-mesoscopic simulation dynamic traffic assignment model. *in ITSC,* 2001.

13. Mahut, M., et al., Calibration and application of a simulation-based dynamic traffic assignment model. *Transportation Research Record*, 2004. Vol.1876(1), p.101-111.

14. Friesz, T.L., et al., A variational inequality formulation of the dynamic network user equilibrium problem. *Operations research*, 1993. Vol41(1), p.179-191.

15. Mahut, M., M. Florian, and N. Tremblay. Application of a simulation-based dynamic traffic assignment model. *The IEEE 5th International Conference on Intelligent Transportation Systems*. 2002.

16. Mahut, M., M. Florian, and N. Tremblay. Traffic simulation and dynamic assignment for off-line applications. *10th World Congress on Intelligent Transportation Systems*. 2003.

17. Mahut, M., M. Florian, and N. Tremblay. Space-time queues and dynamic traffic assignment: A model, algorithm and applications. 82nd Annual Meeting *Transportation Research Board*. 2003.

18. Greenshields, B.D., A study in highway capacity. *Highway Research Board Proc.,* 1935, Vol.1935, p.448-477.

19. Godfrey, J., The mechanism of a road network. *Traffic Engineering and Control*, 1969. Vol.8(8).

20. Daganzo, C.F., Urban gridlock: Macroscopic modeling and mitigation approaches. *Transportation Research Part B: Methodological*, 2007. Vol41(1), p.49-62.

21. Geroliminis, N. and C.F. Daganzo. Macroscopic modeling of traffic in cities. *in Transportation Research Board 86th Annual Meeting*. 2007. No. 07-0413.

22. Edie, L.C., Discussion of traffic stream measurements and definitions. *Port of New York Authority*.1963.

23. Geroliminis, N.D., Carlos F, Existence of urban-scale macroscopic fundamental diagrams: Some experimental findings. *Transportation Research Part B: Methodological,* 2008. Vol.42(9), p.759-770.

24. Keyvan-Ekbatani, M., et al., Exploiting the fundamental diagram of urban networks for feedback-based gating. *Transportation Research Part B: Methodological*, 2012. Vol.46(10), p.1393-1403.

25. Geroliminis, N. and D.M. Levinson, Cordon pricing consistent with the physics of overcrowding, *in Transportation and Traffic Theory 2009: Golden Jubilee*. 2009, Springer. p. 219-240.

26. Simoni, M.D., et al., Marginal cost congestion pricing based on the network fundamental diagram. *Transportation Research Part C: Emerging Technologies*, 2015. Vol.56, p.221-238.

27. Knoop, V., S. Hoogendoorn, and J. Van Lint, Routing strategies based on macroscopic fundamental diagram. *Transportation Research Record*, 2012. Vol.2315(1), p.1-10.

28. Yildirimoglu, M., M. Ramezani, and N. Geroliminis, Equilibrium analysis and route guidance in large-scale networks with MFD dynamics. *Transportation Research Procedia,* 2015. Vol.9, p.185-204.

29. Daganzo, C.F. and N. Geroliminis, An analytical approximation for the macroscopic fundamental diagram of urban traffic. Transportation Research Part B: Methodological, 2008. 42(9): p. 771-781.

30. Geroliminis, N. and B. Boyacı, The effect of variability of urban systems characteristics in the network capacity. *Transportation Research Part B: Methodological*, 2012. Vol.46(10), p.1607-1623.

31. Leclercq, L. and N. Geroliminis, Estimating MFDs in simple networks with route choice. *Procedia-Social and Behavioral Sciences*, 2013. Vol.80, p.99-118.

32. Buisson, C. and C. Ladier, Exploring the impact of homogeneity of traffic measurements on the existence of macroscopic fundamental diagrams. *Transportation Research Record*, 2009. Vol.2124(1), p.127-136.

33. Cassidy, M.J., K. Jang, and C.F. Daganzo, Macroscopic fundamental diagrams for freeway networks: Theory and observation. *Transportation research record*, 2011. Vol.2260(1), p. 8-15.

34. Courbon, T. and L. Leclercq, Cross-comparison of macroscopic fundamental diagram estimation methods. *Procedia-Social and Behavioral Sciences*, 2011. Vol.20, p.417-426.

35. Ji, Y., et al., Investigating the shape of the macroscopic fundamental diagram using simulation data. *Transportation Research Record*, 2010. Vol.2161(1), p.40-48.

36. Geroliminis, N. and J. Sun, Properties of a well-defined macroscopic fundamental diagram for urban traffic. *Transportation Research Part B: Methodological*, 2011. Vol.45(3), p.605-617.

37. Laval, J.A. and F. Castrillón, Stochastic approximations for the macroscopic fundamental diagram of urban networks. *Transportation Research Part B: Methodological*, 2015. Vol.81, p. 904-916.

CHAPTER 3

ANALYSIS OF FLOOD PROBLEMS IN BANGKOK

This chapter provides an overview of flood risks in the study area associated with precipitation and drainage capacity, to better understand present and future flood vulnerabilities of infrastructures associated with different scenarios. Impacts of flooding on transportation networks are also estimated. Flood hazard maps are generated to identify critical infrastructure nodes at risk. Results suggest progressively increased risks of fluvial flooding impacting important infrastructure.

3.1 Flood risk area

Short-duration surface water flooding in the Bangkok Metropolitan Region (BMR) occurs on an annual basis during rainy seasons. The risks could be further intensified in a changing climate with more intense rainfall episodes, especially for low-lying areas with a high rate of land subsidence [1]. The BMR is vulnerable to surface water flooding due to its low-lying topography, intense rainfall episodes during the monsoon season and sub-standard drainage capacity design.

The study of Duangyiwa [2] presented surface water flood modeling work undertaken in the Sukhumvit area, one of the Central Business Districts in Bangkok. Present and future surface water flood risks were evaluated related to rainfall episodes of various magnitudes and distributed land subsidence. Land level changes impact the efficiency of drainage systems in the region and flow dynamics on the floodplain. This study used the 2-hour historical record in Bangkok on 1st July 2011 as a baseline event for future scenario design and considered the land subsidence rate for the period 2005 to 2010 continued up to 2100, with the same spatial pattern [1]. Time-series of rainfall were constructed by calculating the peak intensity and reconstructing the rainfall profiles before and after the peak across the relevant spectrum durations for different return periods [3]. This allowed the generation of rainfall photographs of various return periods (1, 2, 5, 10, 20, 50, and 100 years) using the historical records at Wattana Station.

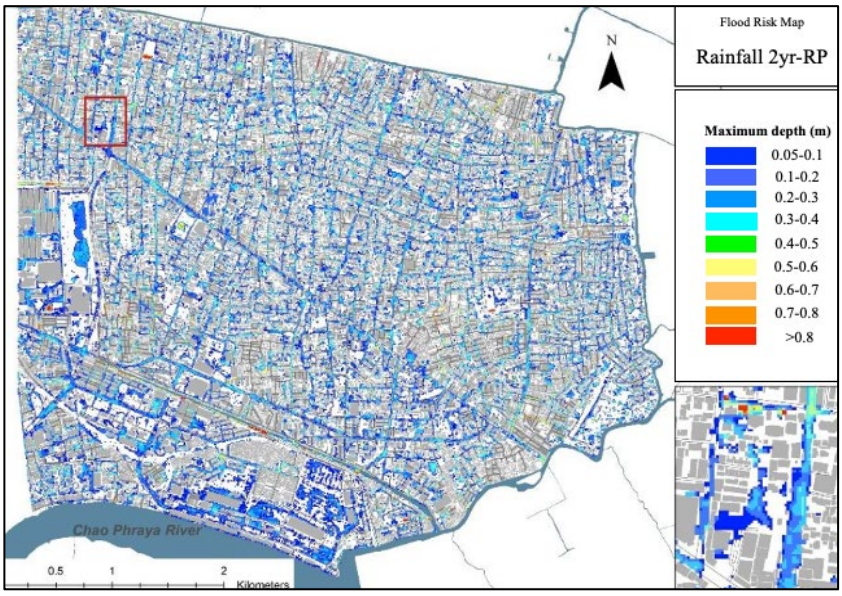

Figure 3.1 Flood hazard map associated with the 2 years return period rainfall scenario

Surface water flood modeling [2] in the Figure 3.1 shows a flood hazard map for a 2-year return period rainfall scenario on 2011 topography, along with critical infrastructure nodes. A threshold depth of 0.1 m was applied in the evaluation. A 10 cm water depth posed no major risks to buildings but caused traffic congestion across the BMR, with road networks affected by floods. Table 3.1 presents the total number of roads affected by the annual return period rainfall. Total road length in the study area is 428.4 km.

Table 3.1 Summary of roads affected in different scenarios in study area.

Scenario	Total affected road	
	Distance (km)	Percent (%)
RT-2yr	146.4	34.2%
RT-5yr	179.3	41.9%
RT-10yr	196.1	45.8%
RT-20yr	209.4	48.9%
RT-50yr	222.5	51.9%
RT-100yr	234.0	54.6%

In Bangkok, average total annual rainfall, as measured by the Thai Meteorological Department, is in excess of 2,000 mm. Frequent road flooding also occurs in various areas even where rainfall does not cause major floods. Historical rainfall data collected from 131 meteorological stations installed around Bangkok are shown in Figure 3.2. Raster maps were generated to compare the amount of rainfall. Rainfall distribution was more spatially

concentrated in the central business district (CBD), leading to increased risk of urban flooding.

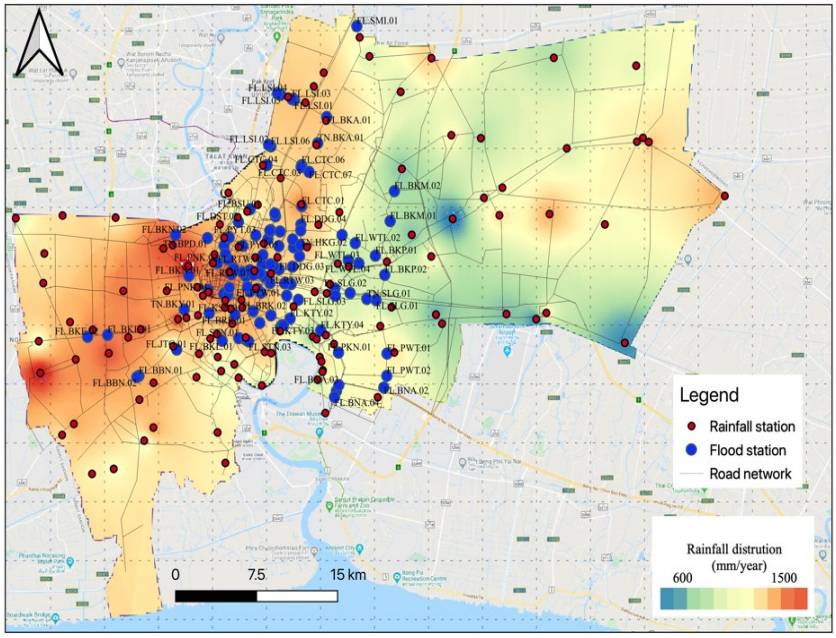

Figure 3.2 Locations of rain stations and flood stations in Urban Bangkok

3.2 Flood risk road

The 2019 statistical data of maximum road flood depths, with detectors installed to monitor flood conditions on roads and tunnels in Bangkok is shown in Figure 3.3.

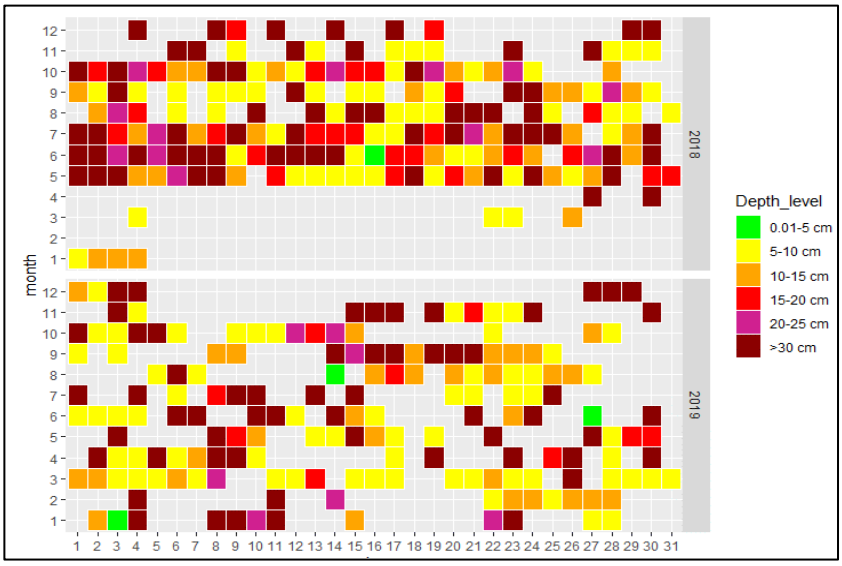

Figure 3.3 Maximum flood depth in the Urban Bangkok

Figure 3.4 shows road flood risks in Bangkok by considering the cumulative average rainfall criteria. When average rainfall accumulated at less than 60 mm/hr, 14 flooded areas occurred, while rainfall at over 60 mm/hr gave 56 flooded areas.

Figure 3.4 Flood risk road

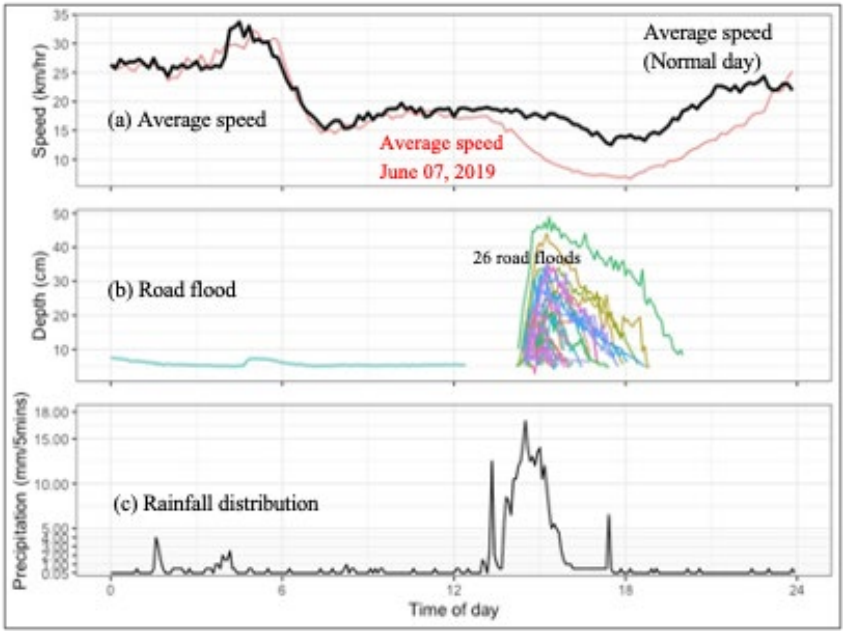

Figure 3.5 Rainfall events on June 07, 2019.

On June 7, 2019 heavy precipitation in Bangkok resulted in the flooding of 26 roads in 14 areas causing traffic congestion [4]. The impact of road floods on average vehicle speed is shown in Figure 3.5.

Average vehicle speed during a normal rush hour is almost the same as the average speed when flood depth occurs at less than 10 cm. Thus, average speed of travel during rush hours is unaffected when the flood depth is less than 10 cm. Conversely, when the flood depth is more than 10 cm during rush hour, average traveling speed is reduced. It takes around 3 hours to drain the roads when rainfall intensity exceeds 5 mm/5min. Research by Hilly et al. [5] investigated the impact of waterlogged roads in the Sukhumvit area of Bangkok by interviewing motorcyclists, taxis, small pick-ups, and buses to identify the relationship between water depth and vehicle speed. Results showed that flooding at a depth of 30 cm and above caused traffic congestion in the Sukhumvit area. This finding was consistent with Pregnolato et al. [6]. They combined data from experiments and observations to create a depth-disruption function that related flood depth with vehicle speed. Using their model, an average depth of 30 cm reduced travel speed to 0 km/h as the ultimate threshold for safe driving of most vehicles.

3.3 Case Study

The study was conducted in the Sukhumvit area (Figure 3.6) located in the eastern sub-urban part of Bangkok. This area is 22.68 km^2 and consists of the Wattana and Klong Toei administrative districts. Total population in the two districts is 191,328. Sukhumvit is geographically located at 13°44'18.01"N latitude and 100°33'41.31"E longitude.

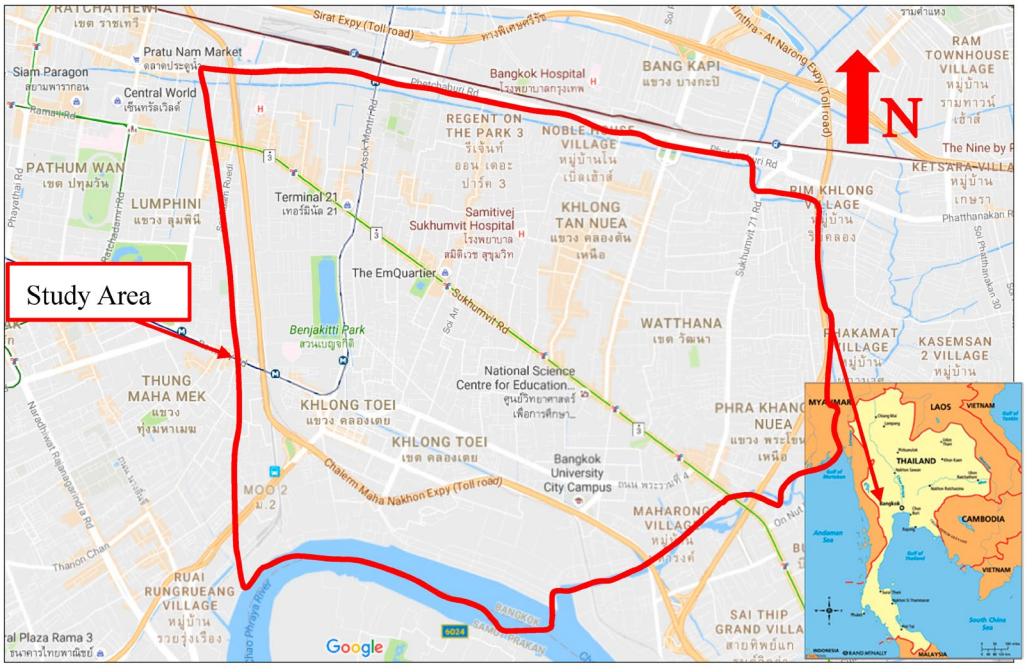

Figure 3.6 Map of Sukhumvit Area

The area is flat, with an average altitude of 0.4 m to 1 m above mean sea level on the eastern and northern sides which connect to the Chao Phraya River on the southern side. There are four major highways as Rama IV Road, Sukhumvit Road, and Asoke Montri Road, five Bangkok Mass Transit System-BTS Skytrain stations (Nana, Asoke, Phrom Phong, Akamai, and Phra Khanong) and the Sukhumvit MRT underground station. The Sukumvit area is flat and gravity discharge of stormwater takes time. Pumps are used to move water to the main drainage system. The existing network is combined with the sewer system. Primary drainage in Bangkok consists of 10 polders as the secondary drainage system (Department of Drainage and Sewerage, DDS). Ingress of floodwater from outside is prevented by pumping stormwater out of the area to the main drainage sites. Sukhumvit withstood the fluvial floods caused by the Chao Phraya River overflowing in 1995 and 1996 [7].

REFERENCES

1. Aobpaet, A., et al., InSAR time-series analysis of land subsidence in Bangkok, Thailand. *International Journal of Remote Sensing*, 2013. Vol.34(8), p.2969-2982.

2. Duangyiwa, C., Modelling future flood risks in the Bangkok Metropolitan Region. *Loughborough University*, 2017.

3. Keifer, C.J. and H.H. Chu, Synthetic storm pattern for drainage design. *Journal of the hydraulics division*, 1957. Vol.83(4), p.1-25.

4. Department of Drainage and Sewerage, B., Flood event recorded in Bangkok, 2019.

5. Hilly, G., et al., Methodological Framework for Analysing Cascading Effects from Flood Events: The Case of Sukhumvit Area, Bangkok, Thailand. *Water,* 2018. Vol.10(1), p.81.

6. Pregnolato, M., et al., The impact of flooding on road transport: A depth-disruption function. *Transportation research part D: transport and environment*, 2017. Vol.55, p. 67-81.

7. Boonya-aroonnet, S., S. Weesakul, and O. Mark, Modeling of urban flooding in Bangkok, in Global Solutions for Urban Drainage. 2002. p.1-14.

CHAPTER 4

ESTIMATING TRAFFIC CONDITIONS BASED ON MACROSCOPIC FUNDAMENTAL DIAGRAM

This chapter presents a research plan aimed at compiling appropriate data for the analysis of flood impacts on the critical MFD parameters free-flow speed, capacity, and jam density. The first step is data collection and selection, and the establishment of data subsets. Datasets are formed by paired samples with both traffic and flood data. The latter must be collected near the test site to accurately reflect flood levels. The final step involves analysis of traffic variables of each flood level on a macroscopic traffic model of urban road networks to investigate the flood impact.

The research methodology process consists of five steps as shown in Figure 4.1.

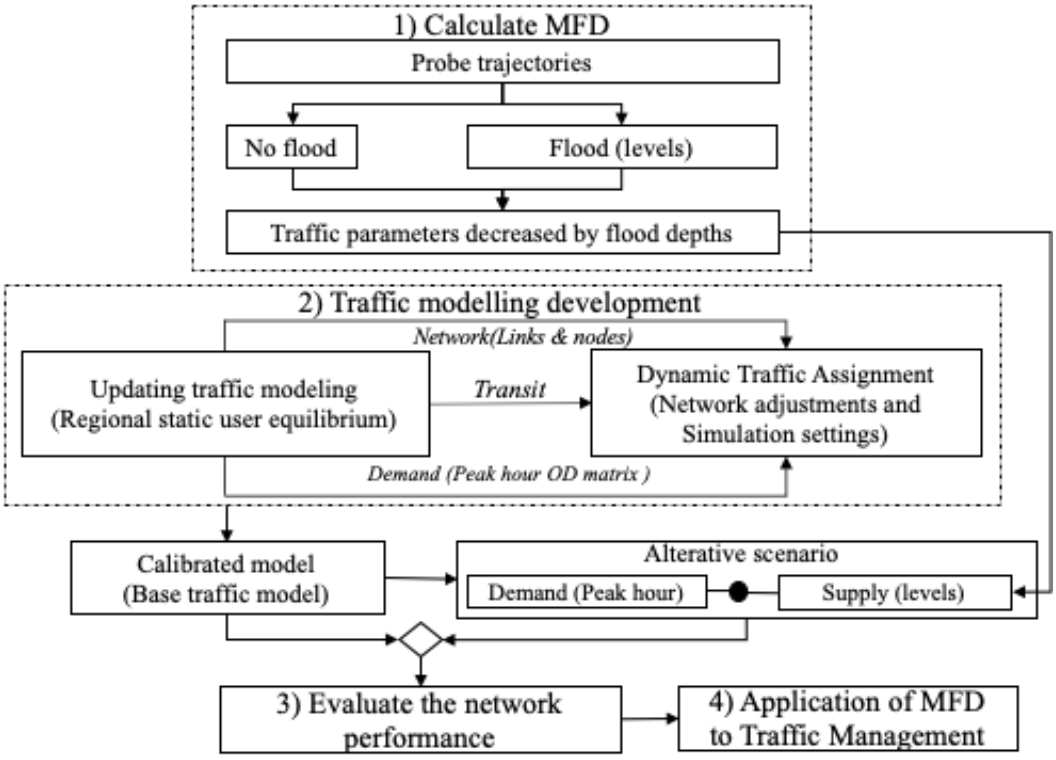

Figure 4.1 Methodological process

4.1 Traffic data

Taxi vehicles equipped with GPS devices that can capture their spatial information are now used to represent vehicle movements in a systematic way. Data are captured and stored every few seconds on a remote server and can be accumulated over a period of months to form a massive knowledge bank with heterogeneous units and data types, referred to as spatial Big Data. Copious information can be extracted by processing this Big Data [1-3].

The Bangkok Metropolitan Administration (BMA) is one of the most taxi-congested cities in the region [4], with 78,078 taxies registered in March 2019. In this study, GPS-equipped taxis in the urban area served as probe vehicles to establish the MFD. To construct the MFD, we used taxi data for 1 year collected in 2019 and obtained as open data (historical raw vehicles and mobile probe data in Thailand) provided by iTIC [5]. Data from 5 a.m. to 12 a.m. on weekdays was included, with no freeway transport. Only taxis that were occupied by passengers were considered because their behavior more closely reflected regular vehicles. Figure 4.2 shows the distribution of the moving points of the taxi in 24 hours. The red boundary represents the Bangkok region and the black boundary encloses the surrounding provinces.

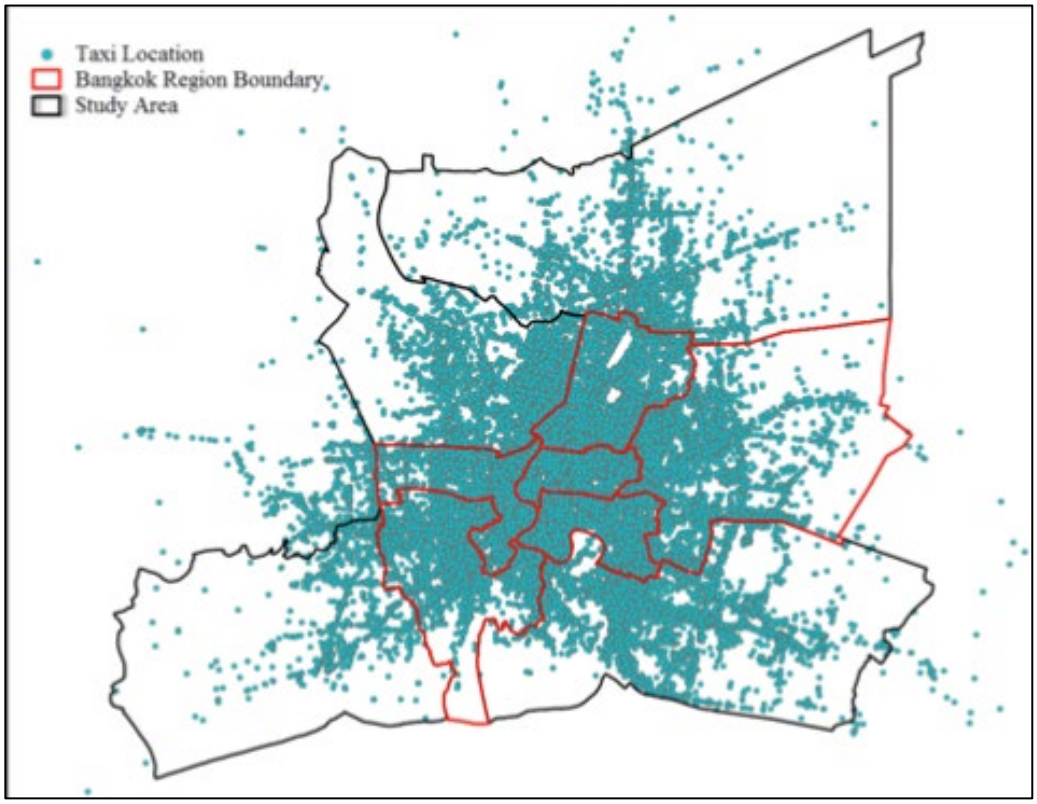

Figure 4.2 Distribution of taxi probe data in 1 day

Probe data of each day were saved in a CSV text file and provided Vehicle ID, GPS Valid, geolocation (longitude and latitude), timestamp (GMT+7), speed (km/h), heading (vehicle heading direction [0-360] degree from North=0), hire light (carrying passenger status), and car key status (active every minute and every 3 minutes). The fields are shown in Table 4.1 with sample data of the taxis in Figure 4.3.

Table 4.1 Data format of taxi probe data collected from GPS-enabled taxis

Column	Data description
Vehicle ID	The unique identification number of each taxi
GPS Valid	1=enough satellite for GPS fix
Lat	Latitude of the taxi position
Lon	Longitude of the taxi position
Timestamp	GPS timestamp (GMT+7)
Speed	Speed of the moving taxi (km/hr.)
Heading	Vehicle heading direction [0-360) degree from North=0
Hire light	Meter shows the status of the taxi meter. (1 = light on or possibly nc passenger, 0 = light off or possibly carrying passengers)
Engine acc	car key status active (1=active, the data will be collected every minute 0=inactive, data collected every 3 minutes)

	VehicleID	gpsvalid	lat	lon	timestamp	speed	heading	for_hire_light	engine_acc
1	ZN2g2qDyrT7FcZ6i8y6EO+47BAs	1	13.78421	100.60486	2019-01-21 00:00:10	30	3	0	1
2	kagOKeh59qBhYy0M6IzJbe44RtM	1	13.78385	100.67363	2019-01-20 23:59:36	53	39	0	1
3	1uI8UkmO56ayZOD9/NFIExmk5jU	1	13.86866	100.66699	2019-01-20 23:59:45	0	168	1	0
4	rzzDns5TPsoibp0iWyY73MVBWDU	1	13.75701	100.63020	2019-01-21 00:00:06	0	346	1	1
5	Pd8LDMgAj+mwPUrbf11SAoE2MQI	1	13.79975	100.63112	2019-01-20 23:57:45	0	278	1	0
6	TdUssqX0C16Q8TFf2FfBM2AbsQo	1	13.82015	100.64478	2019-01-20 23:57:43	0	84	1	0
7	VNkiF3CxmMpATMQncRch7cKYNVc	1	14.33558	100.45425	2019-01-20 23:59:51	0	276	1	0
8	4SyfnF+gSh0sBr1MLbsSurh0tlo	1	13.82716	100.64186	2019-01-21 00:00:14	0	43	1	0
9	3Dja3f1dy0+0YI3TLsuDuvC5C3o	1	13.82085	100.64415	2019-01-21 00:00:02	0	84	1	0
10	VHTtj7iGxRoFsy5Xtz3NbLrZ2ek	1	13.88543	100.71809	2019-01-20 23:59:15	0	179	1	0

Figure 4.3 Sample of taxi GPS log

4.2 Flood data

The Road Flood Monitoring System monitors flood conditions on roads and underpasses in the Bangkok area [reference in] as shown in Figure 4.4. The system operates at 5-minute intervals of data storage frequency and all data are stored for a long time period in the MS SQL database as a very useful tool for road flood forecasting. A total of 94 sensors are installed on important roads throughout urban Bangkok, with 8 sensors in tunnels to measure and display real-time flood graphs.

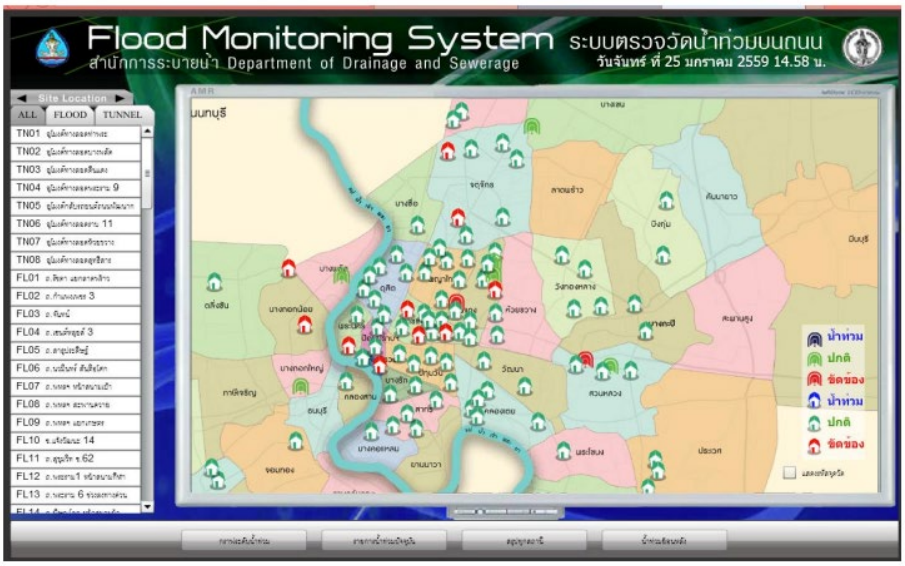

Figure 4.4 Flood station installed in Urban Bangkok

4.3 Estimation of the macroscopic fundamental diagram

Many studies have produced MFDs to estimate the variables of average network flow and density from the fixed detectors' data. However, Leclercq and Trinquier [6] did not recommend flood estimation from these detectors because they cannot capture the spatial dynamics of the links. Vehicle trajectory can produce the MFD very accurately in all network shapes. Therefore, this study estimated the MFD using vehicle trajectories from taxi probes that covered the Bangkok area. A taxi, characteristically, drives randomly with wide distribution, and the destination is determined by the passengers. This conforms to the characteristics of residents' travel and reports their locations as timestamps at every uplink interval. Taxi trajectories were reconstructed on a time-space diagram as shown in Figure 4.5.

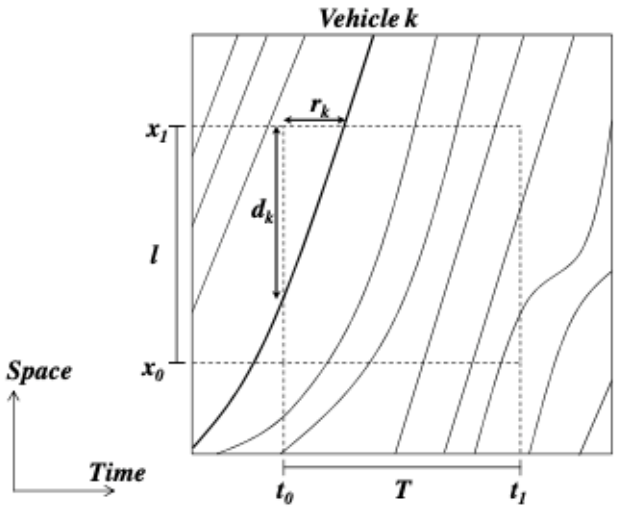

Figure 4.5 Time-space diagram and variables

For vehicle trajectories, the formulas from Edie's definitions [7] based on the two-dimensional diagram presented in Figure 4.5 were used to extract average flow $\bar{q}\imath$ (vehicles/hour), average density $\bar{k}$ (vehicles/km), and average speed $\bar{s}$ (km/h) in the network to obtain the MFD. Let us consider a rectangular region in time and space with dimensions of length of time intervals (T) and total length of all roads in the network (L). Flow and density are defined based on Total Distance Travelled (TDT'_i) and Total Time Spent (TTS'_i), as shown below for section *i*.

$$\mathrm{TDT'}_i = \sum_{\mathrm{i}} \mathrm{d}_{\mathrm{i},k} \tag{4.1}$$

$$\mathrm{TTS'}_i = \sum_{\mathrm{k}} \mathrm{r}_{\mathrm{i},k} \tag{4.2}$$

Where $d_{i,k}$ = the distance traveled by vehicle k in section *i*
$r_{i,k}$ = the time spent by vehicle k in section *i*

Then, the flow and density are defined as:

$$q'_i = \frac{TTS'_i}{n_i \mathrm{l}_i \mathrm{T}} \tag{4.3}$$

$$k'_i = \frac{TDT'_i}{n_i \mathrm{l}_i \mathrm{T}} \tag{4.4}$$

$$s'_i = \frac{\mathrm{TDT'}}{\mathrm{TTS'}} \tag{4.5}$$

Where q'_i = the flow by vehicle in section *i*
k'_i = the density by vehicle in section *i*
n_i = number of lanes in section *i*
s_i = the aggregation interval

Flow and Density of full traffic is estimated as:

$$q_i = q'_i/(X_i) \tag{4.6}$$

$$k_i = k'_i/(X_i) \tag{4.7}$$

Where X_i = the proportion of the number of taxis to full traffic counts in section *i*

Finally, the area average flow (Q) and density (K) are calculated by averaging section variables across an area, according to the following definitions as defined by the following equations.

$$Q = \frac{\sum_i q_i l_i}{\sum_i l_i} \tag{4.8}$$

$$K = \frac{\sum_i q_i l_i}{\sum_i l_i} \tag{4.9}$$

4.3 Result of the macroscopic fundamental diagram

Following previous MFD calculations, the first step was data collection and selection, followed by building relevant data subsets with similar characteristics. These divide the probe data according to road flooding days, by flooding range increased by 5 cm as ranges 0-5, 5-10, 10-15, 15-20, 20-25, 25-30, and over 30. Next, we calculated the flow, density, and speed of each flood range and plotted the relationship between density and flow (Table 4.2), and the relationship between density and speed (Figure 4.6).

Then, this study considered speed to check the relationship of flood range. We compared the means of the speed by analysis of variance to test a hypothesis concerning more than two groups. The ANOVA [8] is a powerful and useful parametric approach to analyze approximately normally distributed data of more than two groups. However, ANOVA does not provide any deeper insights into patterns or comparisons between specific groups. Therefore, we used Tukey's test [9] which compares the means of all treatments to the mean of every other treatment and is considered the best available method in cases when confidence intervals are desired or if sample sizes are unequal.

Table 4.2 Tukey multiple comparisons of speed means

Group	Comparing		diff	lwr	upr	p_{adj}
	Depth1	Depth2				
1	(5-10]	(0-5]	-2.09	-2.95	-1.23	0
2	(10-15]	(0-5]	-4.05	-5.13	-2.96	0
3	(15-20]	(0-5]	-4.80	-6.25	-3.34	0
4	(20-25]	(0-5]	-7.45	-9.09	-5.82	0
5	(25-30]	(0-5]	-7.94	-9.73	-6.16	0
6	(10-15]	(5-10]	-1.96	-2.75	-1.16	0
7	(15-20]	(5-10]	-2.70	-3.96	-1.45	0
8	(20-25]	(5-10]	-5.36	-6.83	-3.90	0
9	(25-30]	(5-10]	-5.85	-7.48	-4.23	0
10	(15-20]	(10-15]	-0.74	-2.169	0.67	0.75
11	(20-25]	(10-15]	-3.40	-5.01	-1.80	0
12	(25-30]	(10-15]	-3.89	-5.65	-2.14	0
13	(20-25]	(15-20]	-2.65	-4.53	-0.78	0
14	(25-30]	(15-20]	-3.14	-5.15	-1.14	0
15	(25-30]	(20-25]	-0.489	-2.63	1.65	0.99

Table 4.2 shows Tukey's multiple comparisons of means at 95% family-wise confidence level and the adjusted p-values for all possible pairs. The confidence levels and p-values only showed significance for between-group differences of depth 1 and depth 2. Therefore, there were no significant differences in group 10 (sig 0.75>0.05) and group 15 (sig.0.99>0.05). New ranges or depth levels were used to calculate MFD parameters according to flood levels as Dry, 0-5, 5-10, 10-20, and 20-30.

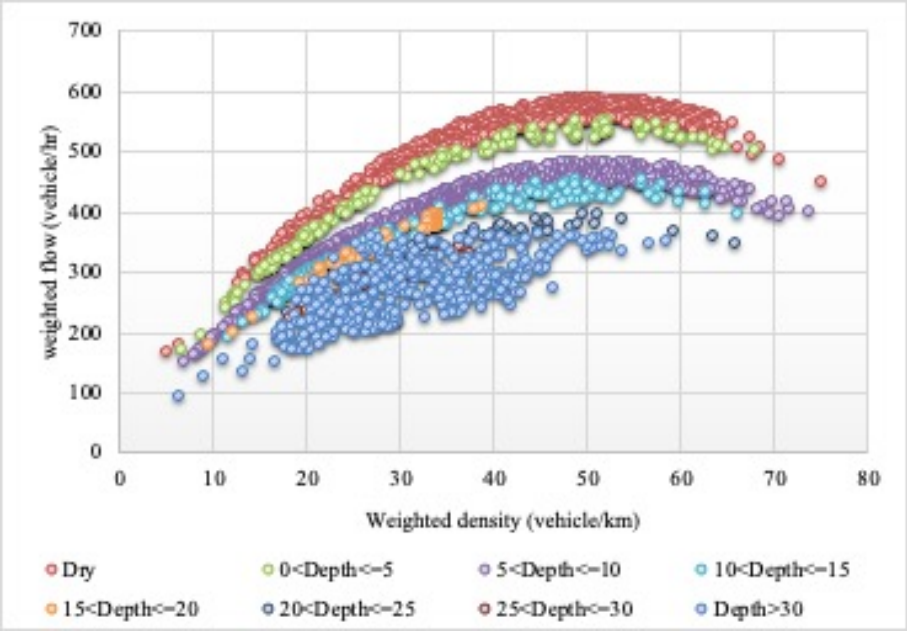

Figure 4.6 Relation of weighted of density and flow under flood levels

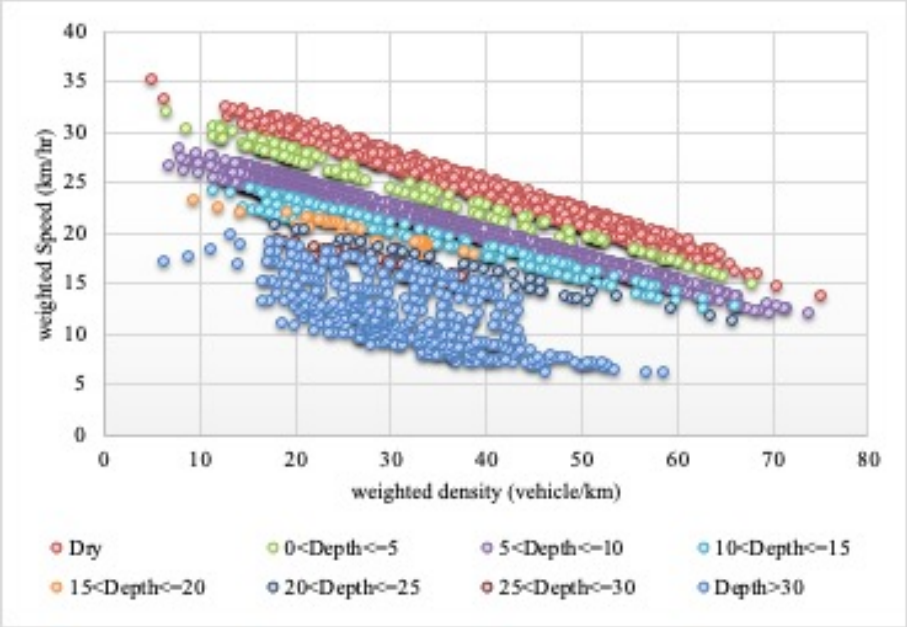

Figure 4.7 Relation of weighted of density and speed under flood levels

The relationships in Figure 4.6 and Figure 4.7 show MFD shape as a change in the traffic operation of the networks under different flood levels. Varying degrees of impact make the MFD shape change and scatters occur. The dry condition had different degrees of impact on the stability and certainty of the road network. Flood levels of less than 5 cm only slightly affected the MFD shape change, with clear differences in MFD shape change for flood levels from 5 to 20 cm. Flood levels exceeding 30 cm had a greater effect on the discrete shape of the MFD.

Table 4.3 shows an equation describing the relationships between macroscopic traffic variables such as density, flow and speed under different flooding depths. The R-square values of fitting MFD curves under each flooding depth and the state turning point are also given. The coefficient of determination, R-square is the statistic of the goodness of fit and can be used to describe discrete changes in the MFD. We found that the R-square value reduced as flood depth increased, while continuity also decreased. R-square of fitting MFD curves under each flood level and the state turning point are also given. For smaller R-square values, more discrete changes were shown by the MFD.

Table 4.3 Equation of macroscopic traffic variables

Depth (cm)	Density-Flow		Density-Speed	
	Equation	R_{square}	Equation	R_{square}
Dry	$y = -0.1968x^2 + 20.283x + 47.39$	0.97	$y = -0.2927x + 35.90$	0.98
(0,5]	$y = -0.181x^2 + 18.749x + 51.92$	0.95	$y = -0.2688x + 32.88$	0.98
(5,10]	$y = -0.1582x^2 + 16.342x + 41.38$	0.93	$y = -0.2352x + 29.05$	0.96
(10,20]	y = -0.1437x2 + 14.988x + 43.54	0.92	$y = -0.2172x + 26.41$	0.91
(20-30]	y = -0.1271x2 + 13.528x + 18.90	0.90	$y = -0.1722x + 22.24$	0.82

The equation relation in Table 4.3 is similar to the Greenshields' model of linking traffic. The fitting curves obtained can offer the value of many key parameters used to quantitatively master and evaluate the traffic state of the study network. The equations were obtained by analyzing and fitting the parameters of Greenshields [10] such as free-flow speed (u_f), maximum flow (q_c) and traffic jam density (k_j). Results of the key traffic-flow parameters are presented in Table 4.4.

Table 4.4 Results of fitting macroscopic traffic variable equations

Depth (cm)	Free flow speed (km/hr.)		Maximum flow (veh/hr.)		Jam density(veh/km)	
	Value	%change	Value	%change	Value	%change
Dry	36	-	750	-	122	-
(0,5]	33	-8.3	538	-28.3	122	0
(5,10]	29	-19.4	464	-38.1	126	3.2
(10,20]	26	-27.7	434	-42.1	121	-0.8
(20-30]	25	-30.5	378	-49.6	129	+5.7

REFERENCES

1. RANJIT, S., et al. GPS enabled taxi probe's big data processing for traffic evaluation of Bangkok using Apache Hadoop distributed system. *in Asian Transportation Research Society Symposium*. 2014.

2. Afian, A., A. Odoni, and D. Rus. Inferring unmet demand from taxi probe data. *18th International Conference on Intelligent Transportation Systems.* 2015.

3. Dimitriou, L., et al., Dynamic estimation of optimal dispatching locations for taxi services in mega-cities based on detailed GPS information. *IFAC-Papers Online*, 2016. Vol.49(3), p.197-202.

4. Department of Land Transport, *Number of Vehicle Registered in Thailand [cited 2020 30 October 2020]*; Available from: https://web.dlt.go.th/statistics/.

5. The Intelligent Traffic Information Center Foundation (iTIC), Historical Raw Vehicles and Mobile Probes Data in Thailand. 2020.

6. Leclercq, L., N. Chiabaut, and B. Trinquier, Macroscopic fundamental diagrams: A cross-comparison of estimation methods. *Transportation Research Part B: Methodological,* 2014. Vol.62, p.1-12.

7. Edie, L.C., Discussion of traffic stream measurements and definitions. *Port of New York Authority.* 1963.

8. RM, C.J.F.A.H., Analysis of variance; designed experiments. *JM Chambers and TJ Hastie (eds.)*, 1992.

9. Yandell, B.S., Practical data analysis for designed experiments. *Crc Press.* 1977. Vol. 39.

10. Greenshields, B., et al. A study of traffic capacity. *in Highway research board proceedings.* 1935.

CHAPTER 5

DEVELOPMENT OF TRAFFIC MODEL

This chapter describes the process of developing a baseline traffic model from the existing database, as shown in Figure 5.1.

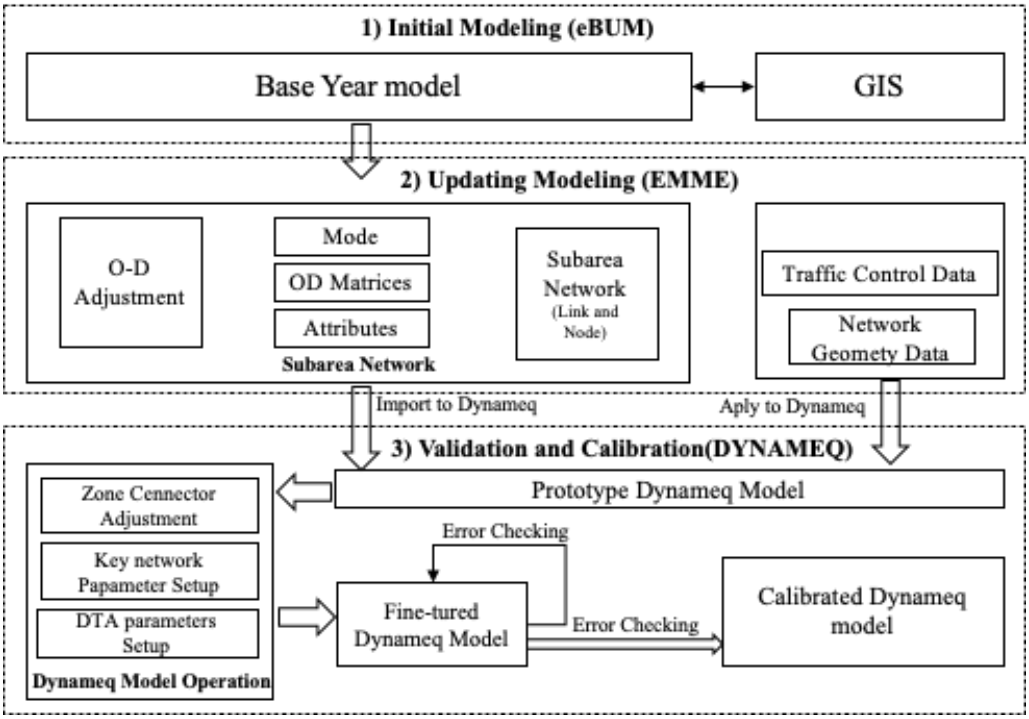

Figure 5.1 Structure of model development

5.1 Initial modeling

Study and review of the extended Bangkok urban model (eBUM) relies on survey data and study results accumulated from previous projects. The eBUM is a strategic model developed by OTP [1] as a baseline to analyze and forecast transport and traffic situation results when changes occur in the transport network study area. To develop the sub-areas, we used data from the OTP's eBUM model (2017) to estimate travel in 2019. This study divided the sub-areas in Bangkok into 500 zones as shown in Figure 5.2 with 7 modes, 17 transit vehicle types, 328 transit lines, 2,033 regular nodes, 25,230 transit line segments, and 7,230 directional links.

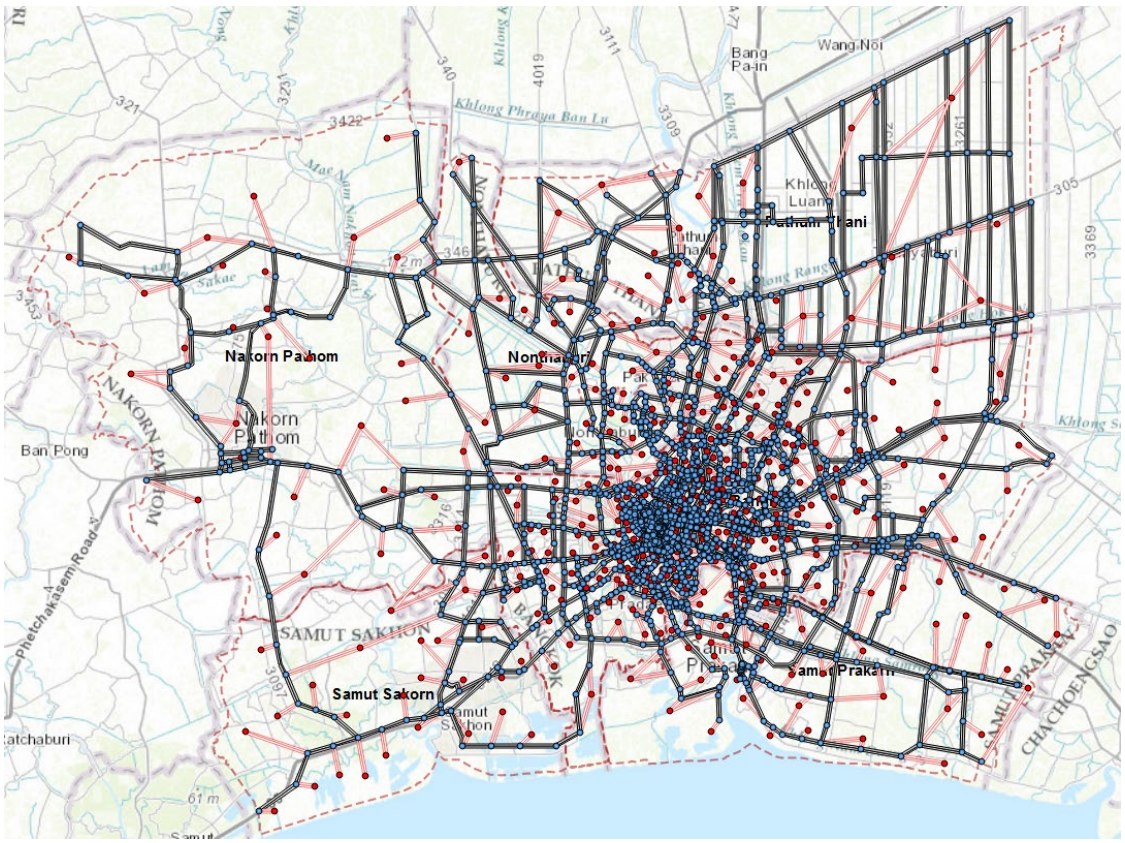

Figure 5.2 Extended Bangkok urban model (eBUM)

Transport forecasting included transport plans and projects of relevant agencies as well as future mass rapid transit projects to analyze future traffic situations. Analysis results are illustrated in Tables 5.1-5.3.

Table 5.1 Forecasted proportion of main trip with public transport system

Unit: 1,000 person-trip/day

Year	Total	Private	Private (%)	Public	Private (%)
2012	22,796	14,647	64.25	8,151	35.75
2013	25,424	17,074	67.16	8,351	32.84
2017	27,618	19,110	69.19	8,508	30.81
2019	28,253	19,410	68.70	8,843	31.30
2022	30,320	21,272	70.16	9,047	29.84
2027	32,986	23,410	70.97	9,576	29.03
2032	35,764	25,550	71.44	10,214	28.56
2037	38,570	27,780	72.03	10,790	27.97

Source: eBUM

Table 5.2 Forecasted daily traffic

Year	Vehicles-distance of travel (VDT)			Vehicles-time of travel (VHT)		
	Morning	Evening	All day	Morning	Evening	All day
2012	14,403,210	13,576,436	183,630,687	694,170	566,714	4,666,342
2013	18,923,014	17,460,370	233,781,354	886,666	718,592	5,963,105
2017	21,653,492	19,942,745	267,036,238	1,197,014	933,898	7,357,397
2019	22,832,096	21,025,165	282,437,353	1,314,852	1,027,047	8,017,695
2022	24,600,003	22,648,795	305,539,025	1,491,608	1,166,771	9,008,141
2027	27,457,154	25,292,018	340,427,690	1,755,838	1,366,411	10,083,075
2032	30,457,445	28,057,431	378,486,075	2,181,860	1,709,719	12,001,841
2037	33,679,692	31,047,970	421,271,012	2,672,468	2,129,595	14,660,999

Source: eBUM

Table 5.3 Major trip proportion categorized by type of travel

Mode		Percent
Private car		68.7%
Public (31.3%)	Bus-air	4.81%,
	Bus non-air	8.02%
	Bangkok Mass Transit System (BTS)	9.62%,
	Mass Rapid Transit (MRT)	4.01%
	Airport Rail Link (ARL)	0.83%
	Boat	4.01%

Source: eBUM

5.2 Updating traffic modelling

To update the traffic model with the most relevant current traffic conditions, we developed a travel network model in urban Bangkok using EMME (Equilibria Multimodal, Multimodal Equilibrium) programs. These are internationally popular and accepted programs for constructing travel network models and network analysis. The EMME program database can be divided into three main parts as shown in Figure 5.3.

1) Network data may be divided into various situations, with each scenario consisting of base networks such as nodes, links, turns, modes, transit vehicles and transit lines

2) Matrices of demand and socioeconomic aspects, and

3) Functions consisting of a set of analysis tools within the model such as volume-delay, transit time, turn penalty, demand, and user defined.

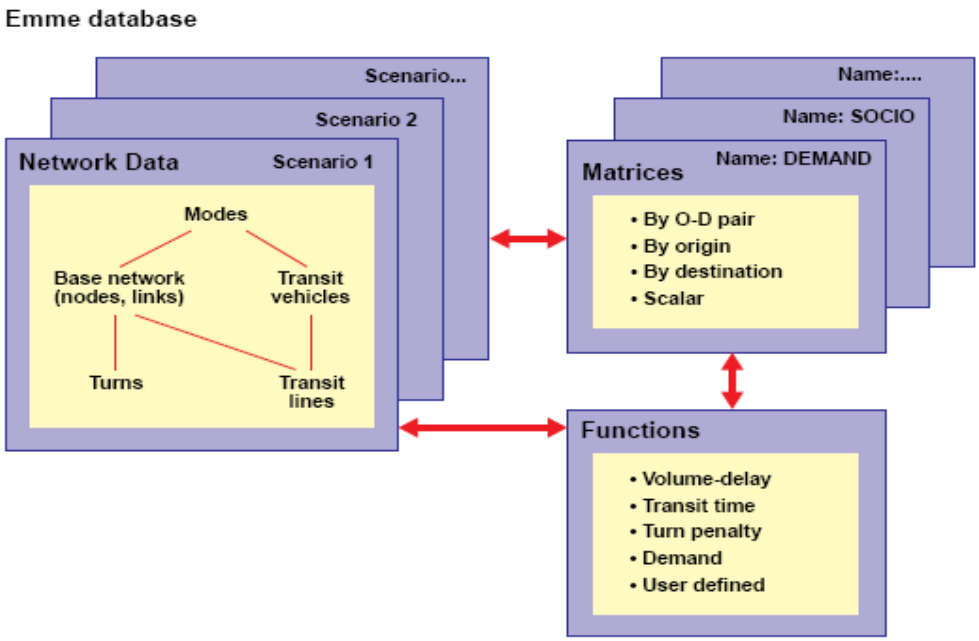

Figure 5.3 Main components of the Emme program

Traditionally, the Bureau of Public Roads (BPR) function is used in models. This curve is based on the 1965 Highway Capacity Manual (HCM) speed-volume relationship, which is parabolic in shape and speed estimates are sensitive to increasing flows. The BPR curve is as follows:

$$t_a = \frac{60L_a}{u_f}\left(1 + \alpha\left(\frac{x_a}{c_a}\right)^{\beta}\right) \tag{5.1}$$

Where
t_a =average travel time on *a* link (minute)
L_a =length on a link (km)
u_f =free-volume speed on *a* link (km/hr)
x_a =assigned traffic volume on *a* link (Passenger Car Unit per hr)
c_a =capacity on *a* link (PCU per hour)
α =the alpha coefficient (0.15)
β =the beta coefficient (4.0)

Using the eBUM model to plan transport, trip data must be adjusted to comply with the latest census as well as reviewing and checking the parameters used in the traffic model. Structure of the process development and implementation of a traffic modeling system is shown in Figure 5.4. Details of the calibration process are described as follows.

1) For each of the zones defined in the Bangkok metropolitan model, trip attraction and trip production matrices are extracted from eBUM (a). Total trips in 2019 from Table 5.1 are updated in these matrices.

2) Evaluate the entropy between each OD pair defined in the network (b). Entropy between OD pair d, E_d is defined as:

$$E_d = exp\left(\frac{u_{fd}}{\overline{u_f}}\right) \tag{5.2}$$

Where u_{fd} = free-flow travel time between OD pair d

$\overline{u_f}$ = the mean of free flow travel time between all OD pairs

With this definition of entropy, an OD pair with short free-flow travel time will give a higher entropy value.

3) A matrix balancing method [2] is adopted in this trip distribution step to find the previous OD matrix (c). In this matrix balancing approach, trip production and attraction data from eBUM (a) are taken as constraints, while the entropy (b) is the weight for distribution. Thus, based on the definition of entropy, more demand is distributed to OD pairs with shorter free-flow travel time.

The previous OD matrix estimated in this step only gives a general pattern of the OD matrix (such as OD pairs with relatively high or low demand) to serve as the starting point of the calibration in the subsequent steps, with no estimation on the level of demand between any OD pairs.

4) The OD matrix from the previous step, which has units in person-trip per day is converted into units of person-trip per hour, consistent with the travel network analysis during rush hours, to calculate the proportion of peak vehicles-distance of travel, as shown in Table 5.2. Then, the OD matrix is split into the previous OD matrices for auto and public transport (d) according to the trip proportions, as shown in Table 5.3.

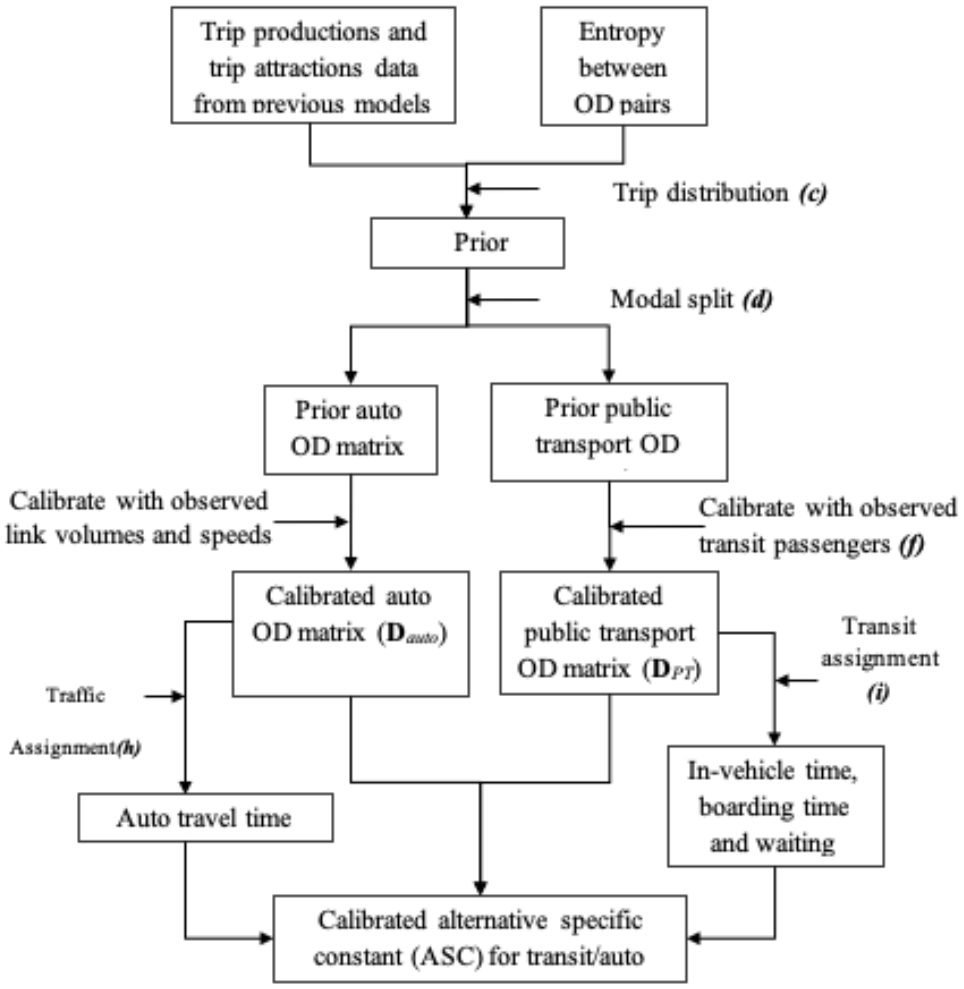

Figure 5.4 Process structure of travel network model calibration

5) The auto OD matrix from the previous step is then calibrated based on observed hourly link count and observed speed (e), which are used to calibrate the auto OD matrix. The observed link speed (s) is converted to the equivalent link volume (V) by rearranging equation 5-3, Currently, 622 links with observed volume data and 956 links with observed speed data are available for use in the calibration. The demand adjustment procedure in EMME, which adopts the gradient approach introduced in Spiess [3], where *le* is the number of lanes with observed link speed.

$$V = le \times 1000 \times \sqrt[3]{(\frac{1}{0.73})(\frac{1.333}{s} - 1)} \tag{5.3}$$

6) The public transport OD matrix from Step 4 is then calibrated based on the observed public transport passenger count (f). This matrix is calibrated after the calibration of auto OD matrix, as the auto link travel time is needed in the transit travel time function for transit assignment.

7) In summing up, the calibrated auto OD matrix (D_{auto}) from Step 5, the calibrated public transport OD matrix (D_{PT}) from Step 6, and the calibrated OD matrix for total travel demand (Q_{travel}) are determined.

8) The calibrated auto OD matrix (D_{auto}) is used to perform auto assignment in EMME to estimate the auto travel time and travel distance between each of the OD pairs (h).

9) The calibrated public transport OD matrix (D_{PT}) is used to perform transit assignment in EMME to estimate the in-vehicle time, boarding time and waiting time for each of the OD pairs (i).

10) With the information from Steps 8 and 9, and the calibrated auto and public transport OD matrices, the alternative specific constant (ASC) for each of the OD pairs for the utility function of private cars (U_{OD}^{PC})and public transport m (U_{OD}^{PT}) can be defined as follows:

$$\mathrm{U}_{\mathrm{OD}}^{\mathrm{PC}} = -\mathrm{GC}_{\mathrm{OD}}^{\mathrm{PC}} \tag{5.4}$$

$$U_{OD}^{m} = -GC_{OD}^{m} - Asc_{OD}^{m} \tag{5.5}$$

Where GC_{OD}^{PC} = the generalized cost of a private car between OD pair

GC_{OD}^{m} = the generalized cost of a public transport m between OD pair

Asc_{OD}^{m} = the fuel cost

The general cost of each mode can be written as an equations as follows.

$$GC_{OD}^{PC} = VT^{PC} \times t_{OD}^{PC} + FC \times d_{OD}^{PC} \tag{5.6}$$

$$G\mathrm{C}_{\mathrm{OD}}^{\mathrm{m}} = \mathrm{VT}^{\mathrm{m}} \times (\mathrm{tvt}_{\mathrm{OD}}^{\mathrm{m}} + \mathrm{bt}_{\mathrm{OD}}^{\mathrm{m}}) + \mathrm{VWT}^{\mathrm{m}} \times \mathrm{wt}_{\mathrm{OD}}^{\mathrm{m}} \tag{5.7}$$

Where VT^{PC} = value of time for travel by private car (2.77 bath/minute)

t_{OD}^{PC} = travel time by private car between OD pair

FC = fuel cost (4 baht/km)

d_{OD}^{PC} = travel time by private car between OD pair

VT^{m} = value of time by public transportation m

Bus-air (1.61 baht/minute)

Bus non-air (1.01 baht/minute)

Bangkok Mass Transit System (BTS) (2.77 baht/minute)

Mass Rapid Transit (MRT) (2.77 baht/minute)

Airport Rail Link (ARL) (2.77 baht/minute)

Boat (1.01 baht/minute)

$\mathrm{tvt}_{\mathrm{OD}}^{\mathrm{m}}$ = in-vehicle travel time public transport m between OD pair

bt_{OD}^{m} = total waiting time spent on taking public transport m between OD pair

VWT = value of time for waiting (3.03 baht/minute)

wt_{OD}^{m} = waiting time of public transport m between OD pair

The above utility functions can be used to calculate the proportion of travel mode (P_{OD}^{m}) between OD pair according to the principles of the Multinomial Logit Model. For example, in the case of private cars (P_{OD}^{PC}) this would be

$$P_{OD}^{PC} = \frac{e^{U_{OD}^{PC}}}{e^{U_{OD}^{PC}} + e^{U_{OD}^{bus-noair}} + e^{U_{OD}^{busair}} + e^{U_{OD}^{BTS}} + e^{U_{OD}^{MRT}} + e^{U_{OD}^{ARL}} + e^{U_{OD}^{Boat}}} \tag{5.8}$$

When the proportion and cost of travel are known between OD pair with the travel mode (m), the Asc_{OD}^{m} of public transport mode m between OD pair can be calculated. For example, a comparison between private car (PC) and buses bus-air is as follows.

$$\frac{P_{OD}^{PC}}{P_{OD}^{Bus-air}} = \frac{e^{U_{OD}^{PC}}}{e^{U_{OD}^{Bus-air}}} \tag{5.9}$$

$$\ln\left(\frac{P_{OD}^{PC}}{P_{OD}^{Bus-air}}\right) = U_{OD}^{PC} - U_{OD}^{Bus-air} - GC_{OD}^{PC} + Asc_{OD}^{Bus-air} \tag{5.10}$$

$$Asc_{OD}^{Bus-air} = \ln\left(\frac{P_{OD}^{PC}}{P_{OD}^{Bus-air}}\right) + GC_{OD}^{PC} - GC_{OD}^{Bus-air} \quad (5.11)$$

Based on the above relationship, any Asc_{OD}^{m} can be calculated from this equation.

$$Asc_{OD}^{m} = \ln\left(\frac{P_{OD}^{PC}}{P_{OD}^{m}}\right) + GC_{OD}^{PC} - GC_{OD}^{m} \quad (5.12)$$

Figure 5.5 and Figure 5.6, these results obtained from the multinomial Logit Model in the Bangkok area as the model developed in the current case (2019). The fixed total demand is considered to be realistic when applied to the case of a road pricing policy. it is assumed that travelers are free to choose between auto and public transport based on the dis utilities they experienced.

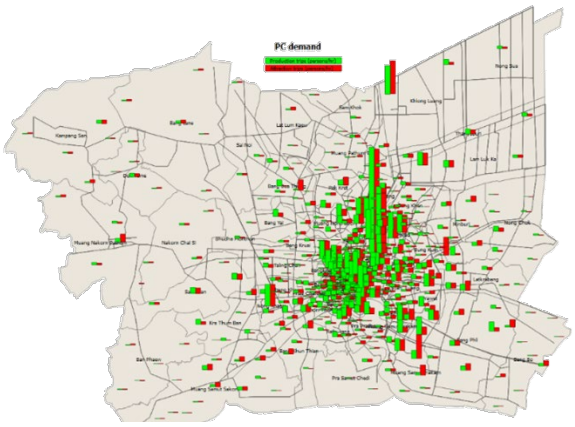

a) Private demand

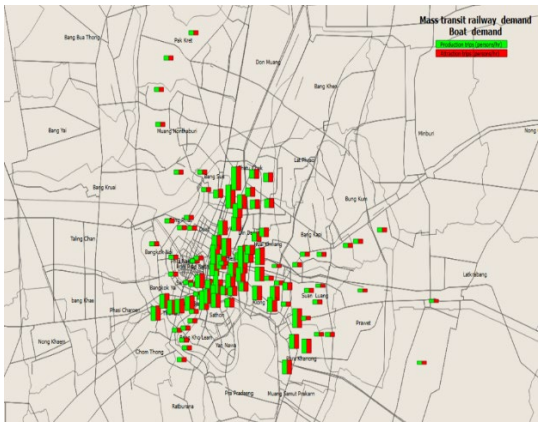

b) Public demand

Figure 5.5 Travel demand

a) Private demand

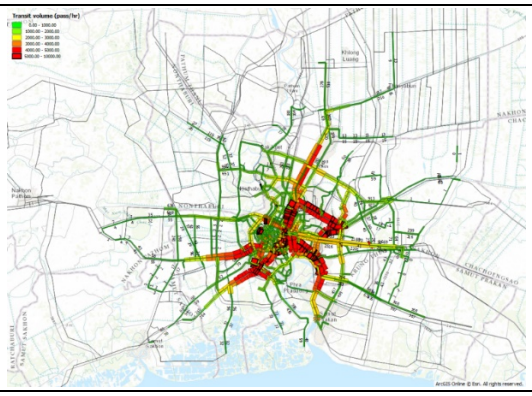

b) Public demand

Figure 5.6 Traffic flow

Figure 5.5 and Figure 5.6 shows the travel demand (person-trip per hour) and corresponding spatial distribution of link volumes (PCU/hour) of the BMA network in 2019. Generally, these figures give the results as expected: high link volumes around the downtown area of Bangkok and a low link volume in the surrounding areas.

5.3 Application of a simulation based on dynamic model

The Mesoscopic model consists of three main elements: traffic demand, network definition, and traffic controls. Traffic demand is represented by one time-dependent OD matrix for each class of vehicles modeled. The representation of the road network is at the level of individual lanes and includes the definition of turn pockets. The permitted lanes for each intersection movement and lane prohibitions by vehicle class are specified where necessary. The network definition does not require lane width or detailed intersection geometry, such as a turning radius. Traffic controls contain all the relevant information regarding the different signaling plans on the intersections. The simulation based DTA model in this study was imported from the eBUM base year model. The imported data included network topology, link, node and turn properties, traffic signal timings, vehicle classes and demand matrices.

5.3.1 Network definition

The network was imported from the eBUM model and included the nodes, the links, and the corresponding centroids of the study area. The nodes represent the intersections of the network and might be either signalized or unsignalized. Based on their type, the priority relationships and the gap acceptance parameters are defined, resulting in the calculation of each movement's capacity. Signalized intersections determine the corresponding actual imposed signal plans. Therefore, priority rules and capacity of each movement are defined based on these signal plans. The links correspond to the roads of the network. Their geometrical characteristics (position, shape, length) and their functional characteristic (free-flow speed) were imported from eBUM model. The capacity of each link was determined based on the three characteristics of free-flow speed of the link, effective length, and response time of each vehicle type. Predefined global values of effective vehicle length and response time were taken as 6.25 meters and 1.25 seconds respectively. The centroids were imported from the eBUM base year model and consisted of the origin-destination (OD) of the conducted trips. Connection of the centroids with the network was established using connectors, carefully placed to be as representative as possible of the actual situation and avoid creating artificial congestion phenomena around

the network. Figure 5.7 shows the created network of the Sukhumvit area, Bangkok as the study area. There were 88 zones, about 207 nodes, 766 links, and 16 traffic signals.

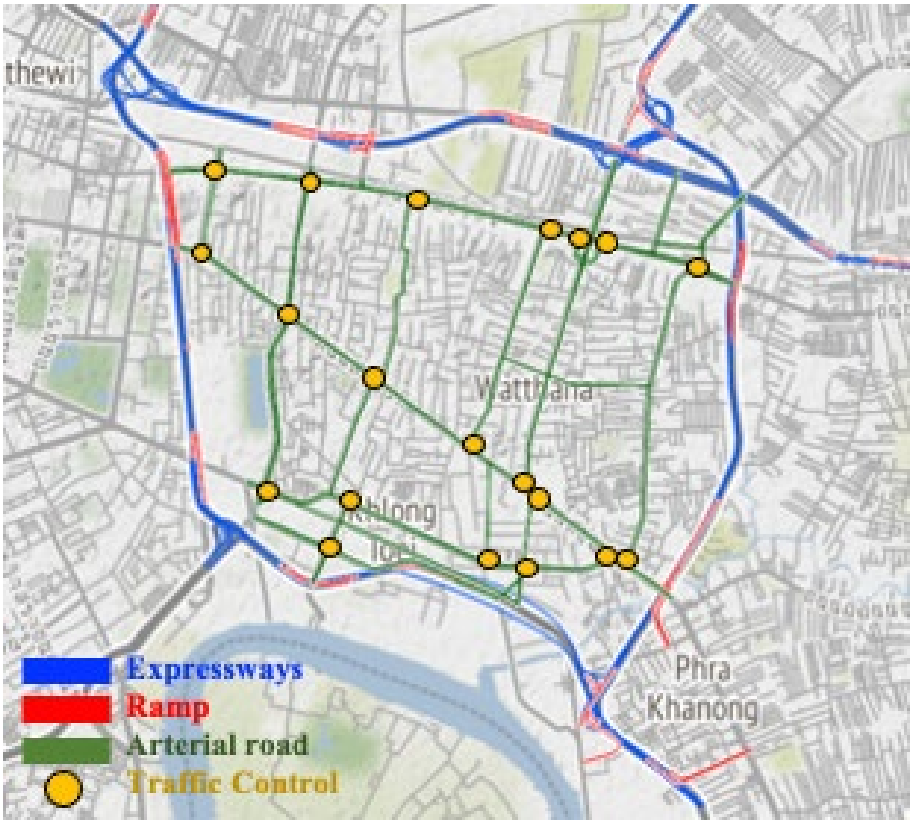

Figure 5.7 Base year model in this study area

5.3.2 General cost functions

The DTA model accounted for intersection delays for streets with stop-controlled intersections but not for delays associated with acceleration and deceleration time. Therefore, the model was adjusted downward to account for acceleration and deceleration time at the stop signs, and the generalized cost function used for path-building was modified to increase the perceived travel time on locals and collectors. This represented the preference for traveling on the arterial system, potentially due to the visibility of the route, or the displeasure associated with stopping at each block.

The generalized cost function was defined by turning movement, facility, penalty (link cost), and toll penalty. Turning movement penalties prevented the abundance of paths from zigzagging across the grid network, the link cost as operating cost included fuel cost and driving cost multiplied by the value of time in this network to arrive (link cost) at an operating cost in units of seconds, while the toll penalty was only used in scenarios that

included congestion pricing. The toll penalty was calculated by dividing the toll cost assigned to a link by the assumed value of time to achieve a time cost, in seconds, of paying a toll. Trips were assigned to the network using the following generalized cost (GC) equation: free-flow speeds on locals and collectors, which have most of the stop signs, were

$$GC = Ptime + LP + RP + FP + Toll \quad (5.13)$$

Where $Ptime$ = generalized cost for movements
LP = left turn penalty (10 seconds)
RP = right turn penalty (30 seconds)
FP = facility penalty (fuel and distance cost) (86.4xlength)
$Toll$ = toll as specified in the scenario (216.6+32.5xlength)

5.3.3 Traffic control

Traffic control plans can be used to assess the impact of different scenarios such as different signal programs. In this study, signal plans were imported from the Control and Command Center (Traffic Police Division, Bangkok). The existing signal plans were not modified, and no further investigation is required regarding this aspect of the model. Figure 5.8 shows simple signal phases scenario. The green times are shown in Table 5.4.

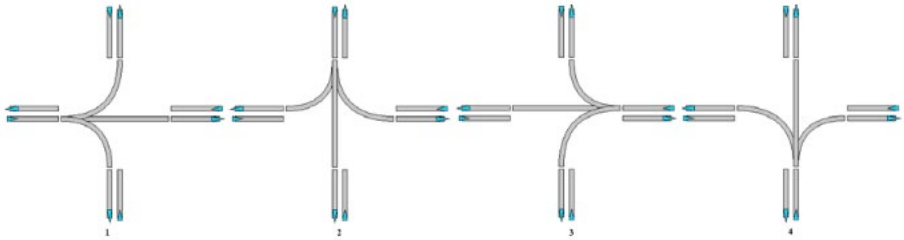

Figure 5.8 Signal phases scenario

Table 5.4 Green, yellow and red times

Signal	Phase (total cycle time:150 sec)			
	1	2	3	4
Green (s)	35	30	35	30
Yellow (s)	3.5	3.5	3.5	3.5
Red (s)	1.5	1.5	1.5	1.5

5.3.4 Geometry

Roadway geometry was sourced from aerial photos (http://map.google.com) together with intersection channelization data. Lane restrictions, turning movement prohibition data and some other issues still needed to be addressed. The network was misaligned with the aerial photo and no intersection geometrical details were coded (pocket lanes, allowed and prohibited movements, movement priority). Nine lanes were coded in zone connectors (representing the unlimited capacity of a connector), while centroid connectors were directly connected to intersections with unrealistic freeway merge/diverge.

5.3.5 Volume

In the Sukhumvit study area, observed volume included 307 locations crossing the road network. Morning peak hour link volume data for links (red bar in Figure 5.9) crossing these screen lines were collected from the BMR.

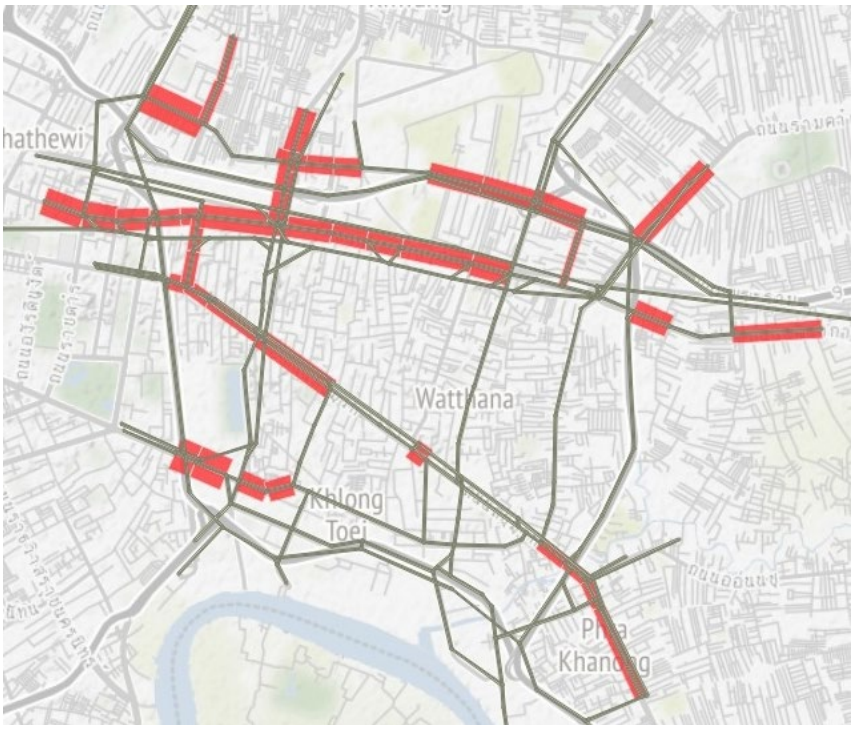

Figure 5.9 Observe flow for model calibration

5.3.6 Traffic demand

The model simulated traffic situations in both the morning period starting at 7:00 and the evening period lasting until 18:30. In each simulation period, a static OD matrix of 1-hour peak was obtained from the eBUM model. The matrix was modified to be dynamic by multiplying by the time step function change. Every hour, the static OD matrix was multiplied by a factor to derive the dynamic OD matrix. The time step function is shown in Figure 5.10.

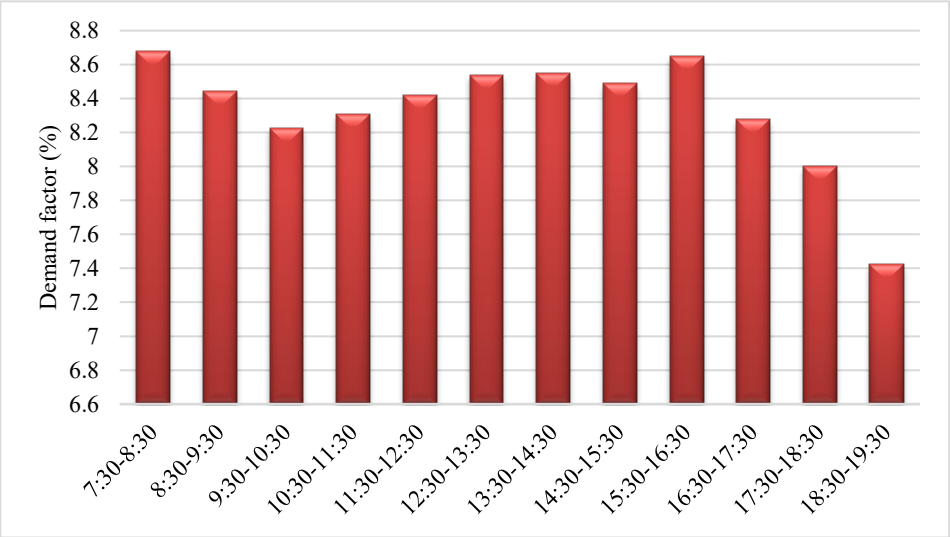

Figure 5.10 Time step function for deriving dynamic OD matrix (eBUM)

When modeling transport, it is normal to focus on dimensions of average weekday peak period for road passenger traffic that are most important; for example, peak hour models are often used because the main interest is in the performance of the transport system when it is under the most pressure.

Therefore, here, we determined only morning peak hour. Imported demand matrices from the eBUM base model include the corresponding OD matrices of private cars calculated from the EMME subarea tool. The demand period covered three hours as suggested by Chiu et al. [4].

1) The study period from 7:30 to 8:30 a.m. is O-D matrices for peak hours.

2) The warm-up period to load the network for the beginning of the analysis period from 7:00 to 7:30 a.m. was 80% of OD matrices for peak hours.

3) The cool-down period to create realistic expectations on the part of drivers as to their travel times from 8:30 to 9:00 a.m. was 80% of OD matrices for peak hours.

4) One hour of the simulation without additional demand, which we monitored for network clearance.

5.4 Calibration and validation

This section provides information relevant to the calibration of simulation based DTA models. The calibration process must be catered to a specific tool and take into consideration its strengths and limitations. A good overview by Chiu et al. [4] covered DTA modeling concepts, including calibration and data-related issues. A 15-minute assignment interval, equivalent to 8 intervals for an assigned OD matrix representing two hours, was used. Up to 20 paths were searched in one assignment interval. Simulation results were collected for one hour in five-minute intervals after the warm-up period. A maximum of 200 iterations with a relative gap of 1% was used as stop criteria. Model results were collected at fifteen-minute intervals for the peak hour only (one hour) starting from peak hour demand loading (30 minutes after simulation started). Hourly aggregated statistics were then calculated. All results reported in the paper were for peak hours only.

5.4.1 Relative gap

If the network cleared, we wanted to find out whether the DTA reached an acceptable state of equilibrium. The relative gap statistic for the last iteration is typical of most interest. The relative gap is the percentage difference in travel times for used paths corresponding to the same departure time interval. In DTA, a relative gap of less than 2% is considered to be good but is not easily achieved in highly congested networks [5].

However, the relative gap only gives an idea of the stability of the current solution and does not quantify the solution with respect to the underlying equilibrium (user-optimal) objective. it indicates that the algorithm is no longer improving the results but does not indicate how well the final solution satisfies the desired objective of equilibrating travel times on alternative paths. Figure 5.11 shows the convergence output from a DTA model in which the initial assignment interval was deemed not converged and the mean value of the relative gap was more than 2% after 40 iterations. The model assignment converged quite well with a mean relative gap value of 2% after 120 iterations.

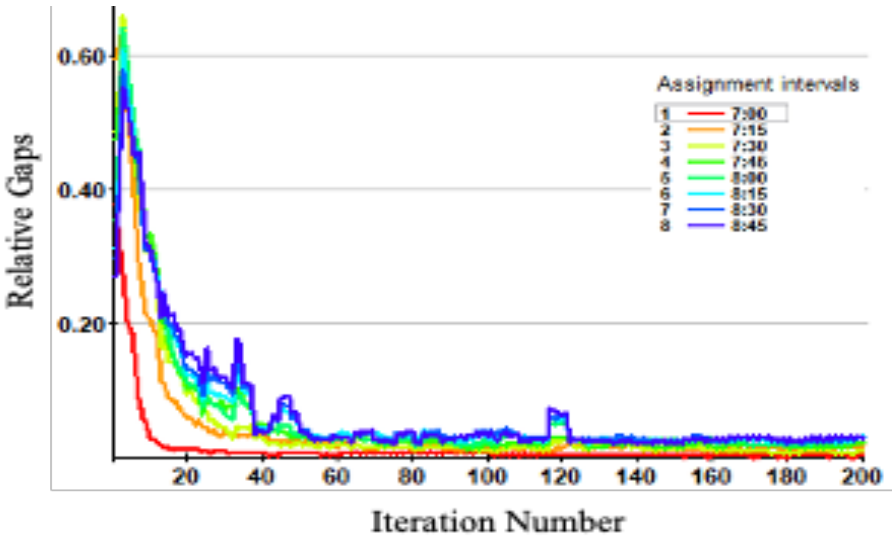

Figure 5.11 Relative gap convergence plot for final base-year assignment

5.4.2 Regression analysis

The Mesoscopic model replicates 2019 morning peak hour (one hour) traffic conditions. Calibration is required to ensure that the model has the capability to replicate traffic volumes, travel time, and other travel patterns in the network. The process involved the calibration of both the demand and supply parts of the model. This was achieved using model volumes and observed counts at the important road segments in the network. Figure 5.12 shows a scatterplot graph to compare model flow and observed flow for the morning peak hours between 7:30 and 8:30. Results indicated that the model was well-calibrated, with R2 of 0.975.

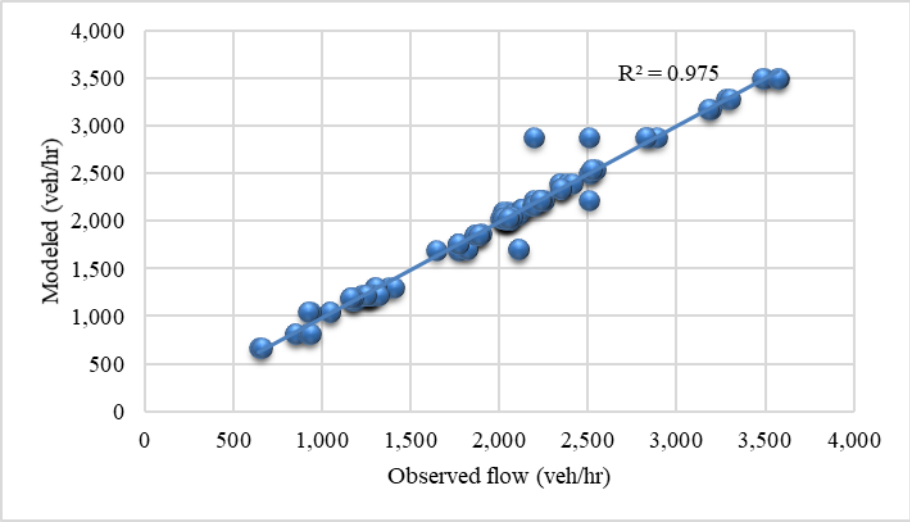

Figure 5.12 Modeled and observed link volumes

5.5 Result of baseline scenario

The initial objectives of this scenario were to obtain a baseline analysis for the morning peak demand period to become the benchmark baseline for subsequent sensitivity analysis scenarios, and to work through the stages of network model development as discussed previously.

5.5.1 Performance indicators

Demand was measured as the total number of vehicle departures during a time interval. Not all of these vehicles were able to enter the physical space of the network and were held as virtual links on the entrance connectors.

In Count measured the number of vehicles that entered the physical space of the network during the time interval, that is, they entered the entrance connectors.

Out Count measured the number of vehicles that exited the physical space of the network during the time interval, that is, they exited from the exit connectors.

Waiting measured the total number of vehicles waiting to enter the network (on virtual links) at the end of the interval. This measure is the difference between the cumulative Demand and In Count values up to that interval.

Traveling measured the total number of vehicles in the network at the end of the interval. This measure is the difference between the cumulative In Count and Out Count measures.

VHT measured the total vehicle-hours (veh-hr) of travel during the interval inside the network. This measure did not include waiting time on virtual links.

VKT measured total vehicle-kilometers (veh-km) traveled during the interval. As with VHT, this did not include vehicles on virtual links.

VHD measured total vehicle-hours (veh-hr) of delay experienced during the interval. This did not include vehicles on virtual links: it reflected the portion of VHT that was delayed by subtracting the portion that represented free-flow travel time.

Average network speed was measured in kilometers during the time interval, derived directly from the VKT and VHT network measures.

Density was measured as vehicles per kilometer per lane (veh/km/lane). Average network density over the time interval considered all vehicles in the physical space of the network, divided by the total km*lane of the network as a time-average of network density over the time interval.

5.5.2 Baseline scenario

Network simulation results are based on link results aggregated to totals or averages for the entire network, as shown in Table 5.5.

Table 5.5 Network results of the baseline scenario

Baseline Scenario	Time Interval				Peak hour
	7:30-7:45	7:45-8:00	8:00-8:15	8:15-8:30	
Demand (veh.)	26,496	26,169	26,374	25,995	105,034
In Count (veh.)	21,414	21,106	20,469	20,773	83,762
Out Count (veh.)	19,585	19,087	18,735	18,774	76,181
VHT (hr.)	2,620	3,076	3,529	3,833	13,059
VHD (hr.)	1,370	1,836	2,282	2,587	8,077
VKT (km)	92,735	91,913	91,662	90,809	367,119
Speed (km/hr.)	35	30	26	24	29
Density(veh/km/ln)	12	14	16	17	15

Once an assignment procedure has run to completion, the first item to check is whether all vehicles have reached their destinations and left the network within a reasonable amount of time after the last demand loads. The relevant outputs are the number of vehicles waiting to enter the network and the number of vehicles remaining in the network at the end of the simulation.

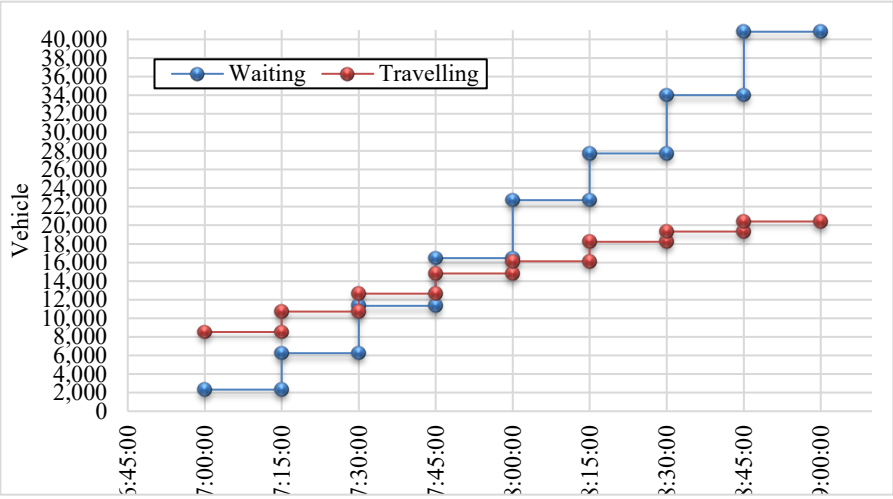

Figure 5.13 Vehicle travel in the road network

Figure 5.13 shows relevant outputs as the number of vehicles waiting to enter the network (on virtual links) and the number of vehicles (traveling) in the network at the end of the interval. The blue line changed suddenly at the third interval (7:45), which is the start of peak hour interval until after the last peak interval demand. Over 25,000 vehicles were waiting to enter the road network. These vehicles were stuck on virtual links and could not get onto the road network to complete their trips.

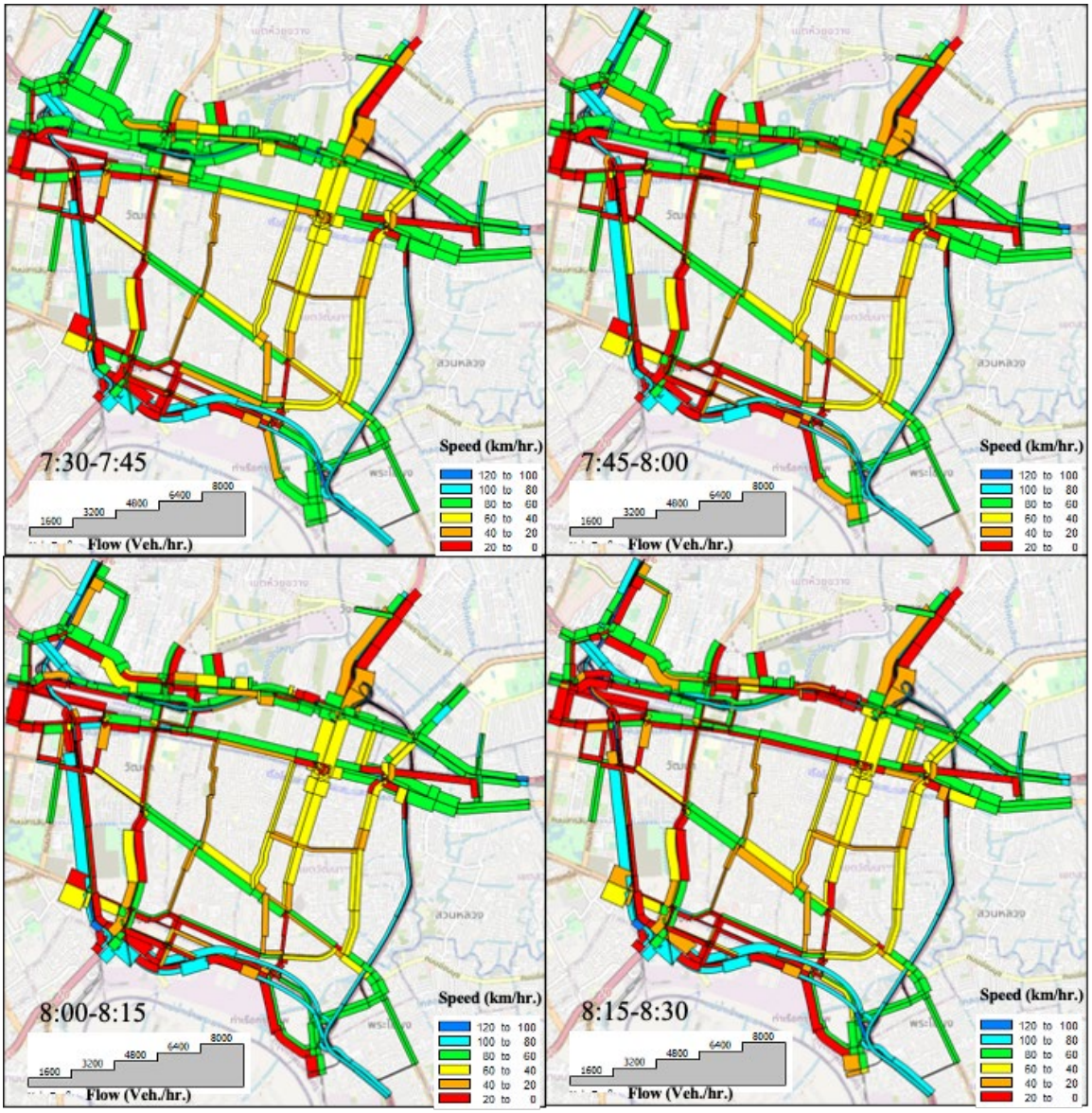

Figure 5.14 Speed and flow of baseline model during morning peak hour

Figure 5.14 shows speed and flow distribution in the network at 15-minute intervals during the morning peak (from 7:30 to 8:30 am) for the baseline scenario. The thickness of the link indicates flow, while color represents speed. Narrow or reduced

thickness links contain flow of 1600 veh/hr with increasing trend in the thickness giving flows of 3200, 4800, 6400, and 8000 veh/hr, respectively. Similarly for speed, red color represents the lowest speed of 0 to 20 km/hr and blue color represents the highest speed of 100 to 120 km/hr. Inner links of the network show almost the same flow and speed for all time intervals but these change in the outer network links. The first 15-minutes shows the highest flow and highest speed but the trend decreases gradually during the subsequent 15-minute intervals as congestion levels increase.

REFERENCES

1. Office of Transport and Traffic Policy and Planning (OTP). *Result of transport and traffic analysis*, 2020. http://mistran.otp.go.th/mis/Interview_HIVOC.aspx.

2. Furness, K.P., Time function iteration. Traffic Engineering and Control, 1965. Vol.7(7), p. 458-460.

3. Spiess, H., A Gradient Approach for the OD Matrix Adjustment Problem. *Centre de Recherche sur les Transports de Montréal: Montréal, Canada*, 1990.

4. Chiu, Y.-C., et al., A primer for dynamic traffic assignment. *Transportation Research Board.* 2010, p.2-3.

5. Gliebe, J. and Å. Bergman, Case Study Evaluation of Dynamic Traffic Assignment Tools. 2011.

CHAPTER 6

ANALYSIS OF IMPACT OF FLOOD ON TRAFFIC CONDITIONS

This chapter investigates the influence of supply and demand on traffic conditions. Demand is assessed as the magnitude and distribution of movements of travelers between different locations when aggregated across the geographical area served by a network, while supply is the physical infrastructure, composed of roads and intersections, and their capacity to efficiently facilitate the movements of travelers.

The approach to transport planning focuses narrowly on problems at a specific location and point in time. This lacks systematic consideration of the characteristics of road traffic networks at a global scale, or how the effects of many individual decisions compound over time. A systematic consideration of the influence of patterns in supply and demand structure on a global scale is requisite for policy interventions to be successfully and effectively transferred between networks with different structures. An understanding of how different configurations of supply and demand structures combine to yield different performance characteristics would be useful for both researchers and policymakers and allow the design of more appropriate and/or effective transport solutions for existing road traffic networks based on their individual structural characteristics.

Therefore, this chapter investigated the perturbations in terms of supply and demand on the simulation results by systematically changing input parameters. Given the uncertainty in model inputs and assumptions, sensitivity analysis can help to build a certain level of confidence to better understand the robustness and resultant reliability of the model.

6.1 Alternative scenarios

Alternative scenarios were developed to accomplish the desired study goals. The first scenario represented the current situation, allowing us to locate possible congestion points around the network. This scenario was used as a basis for comparison with other scenarios. The remaining scenarios were created to enable us to conduct sensitivity analysis, both in terms of supply and demand.

More specifically, overall demand level has increased proportionally by 10 and 20%. To study the effect of increased demand on network performance, the next category

of scenarios included the impact of flood levels on changing MFD parameters as free-flow speed, maximum capacity, and jam density.

This is accomplished by varying the supply parameters of the model. As mentioned before, the type parameters that define the supply part of the model and can vary are the response time and the relative length. The effective length predefined value is set to be equal to 6.25 meters while response time is 1.25 seconds. Any modifications in these two parameters result in a change in the jam density (K_{jam}) and maximum flow rate (Q_{max}) of each link. The free flow speed is the other important component that defines the capacity of the links that the set values are modified according to flood levels. The results of change MFD parameters according to flood depth are displayed in Table 6.1.

Table 6.1 Traffic parameter in traffic model according to flood levels

Water depth (cm)	Free flow speed	Response time (R)	Effective length (L)
0-5	0.92	0.72	1.00
5-10	0.81	0.62	1.00
10-20	0.72	0.58	0.99
20-30	0.69	0.50	1.06

A detailed experimental design of the increased/decreased supply scenarios is presented in Table 6.2.

Table 6.2 Experimental design of alternatives scenarios

Demand OD matrix	MFDs change by flood depth				
	Dry	0-5	5-10	10-20	20-30
0%	Baseline	Scenario3	Scenario6	Scenario9	Scenario12
10%	Scenario1	Scenario4	Scenario7	Scenario10	Scenario13
20%	Scenario2	Scenario5	Scenario8	Scenario11	Scenario14

6.1.1 Result of model convergence

The models simulated the peak hour at full demand, with half an hour for the network to warm up and another half an hour to cool down after peak, with 80% of the peak hour demand. Vehicles in the model were private car class. All models were run with a maximum of 200 iterations and a 1% relative gap. A 15-minute assignment interval, equivalent to 8 intervals for each assigned OD matrix, was used. Up to 20 paths were

searched in one assignment interval. Simulation results were collected every 15 minutes after the warm-up period for one hour.

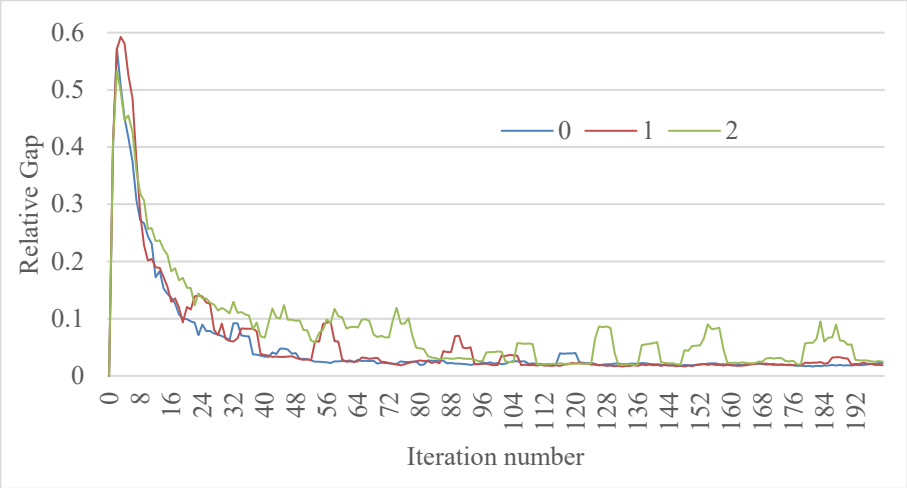

Figure 6.1 Model convergence with different demand levels

Figure 6.1, when demand is increased by 10%, the relative gap gets a modest but noticeable increase. With 20% increase in demand, the model generates more fluctuations, and the relative gap goes higher, indicating the network is more congested so that traffic between an O-D pair switches back and forth among a few alternative routes.

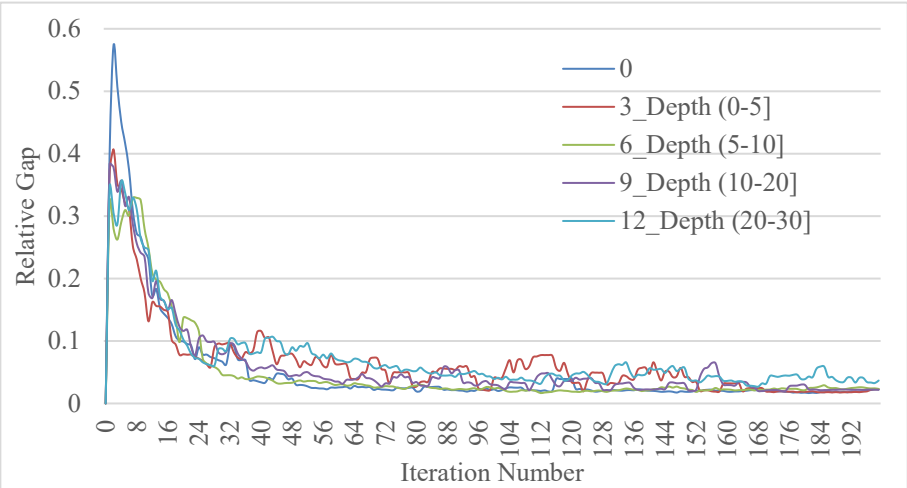

Figure 6.2 Model convergence with different flood depths

Figure 6.2, when MFD parameters changed, model convergence patterns were similar and convergence curves closely matched. This indicated that in terms of network convergence, the model was more sensitive to the demand change than MFD parameter changes.

6.1.2 Results of alterative scenarios

Vehicle kilometers traveled (VKT) and Vehicle hours traveled (VHT) during the peak hour were selected as two major performance measures of effectiveness (MOE) in the elasticity calculation [1]. VKT is regarded as a benchmark of network utilization, i.e., how much traffic can be served in the system. When demand increased, more vehicles traveled in the network and VKT increased; however, in peak hour this did not hold because VKT and VHT were determined by vehicles that had completed their trips. Due to network congestion, the number of exited vehicles (vehicles that had been served) stabilized when system throughput reached capacity, while demand continued to increase.

After this point, VKT in peak hours did not greatly change, no matter how high the demand. VHT is regarded as a benchmark of network efficiency. Lower VHT means that the system is operating more efficiently. Unlike VKT, VHT will always increase when the network becomes more congested.

Elasticities of VKT and VHT were calculated with the following formula:

$$Elasticity = \frac{\%MOE}{\%input} \tag{6.1}$$

Where $\%MOE$ = percent change demand in VKT or VHT each flood scenario

$Input$ = percent change in demand each flood depth

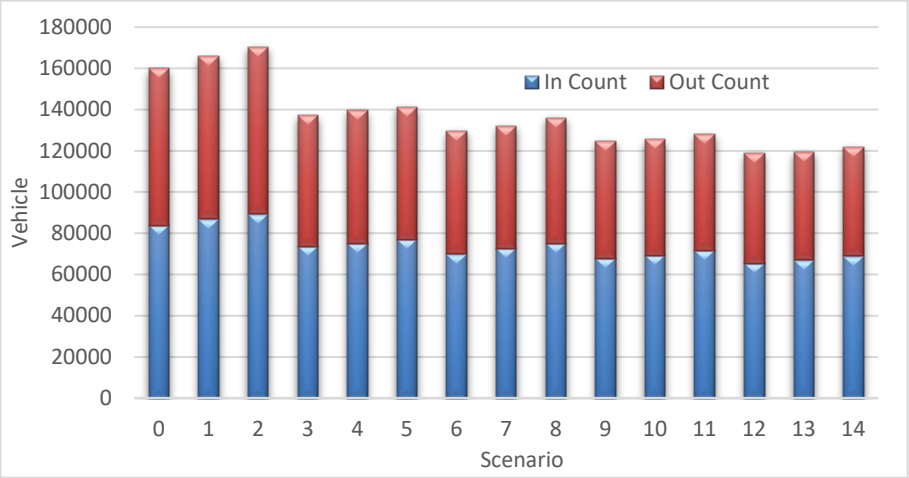

Figure 6.3 Number of vehicles entering and exiting in the network

Figure 6-3 shows the number of vehicles entering and exiting from the network. The number of vehicle entries and exits in all scenarios increases with increasing demand, while the flooding scenarios show a decrease from the baseline scenario to high depth scenario. This occurs because the number of trips by entering vehicles reduces. On the other hand, for exiting vehicles, congestion in the network is high and vehicle movement decreases. Most of the vehicles cannot reach their destination on time.

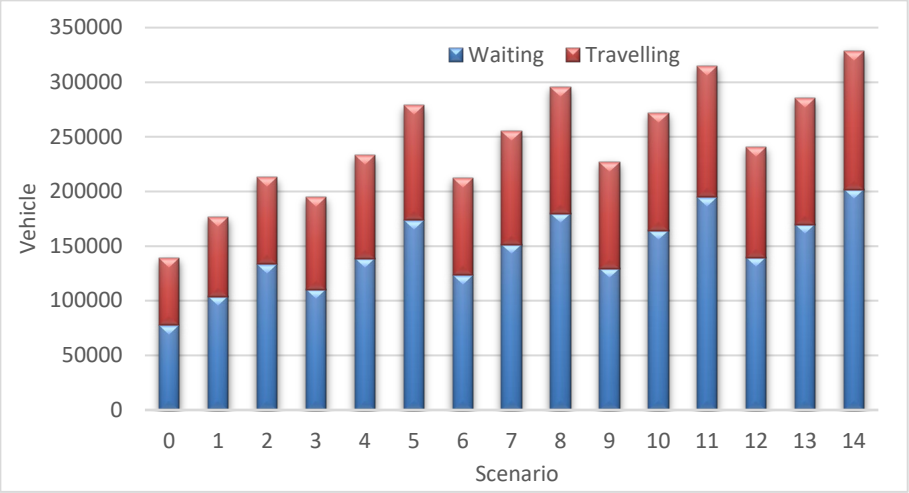

Figure 6.4 Total number of vehicles waiting and traveling in the network

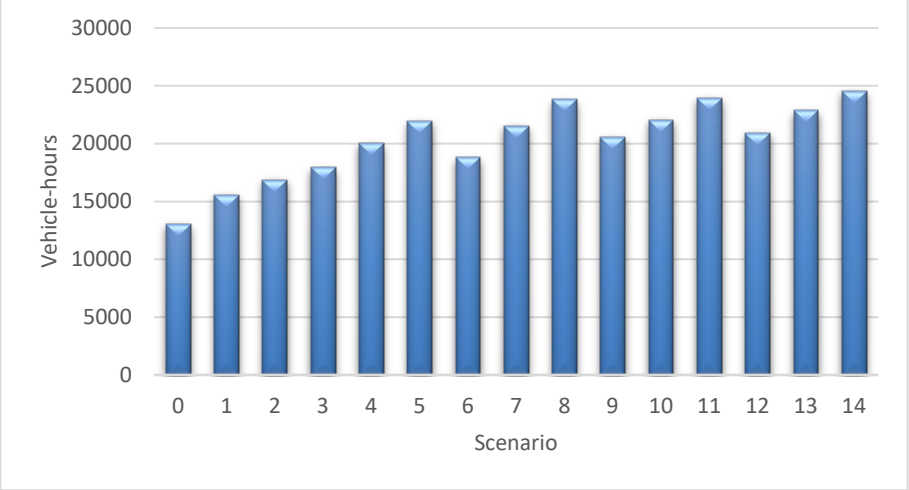

Figure 6.5 Total vehicle-hours traveled

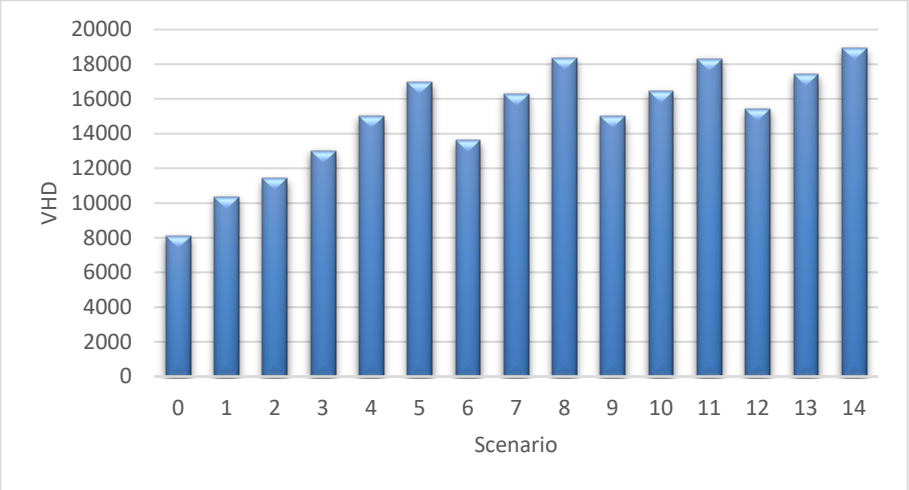

Figure 6.6 Total vehicle-hours of delay experience

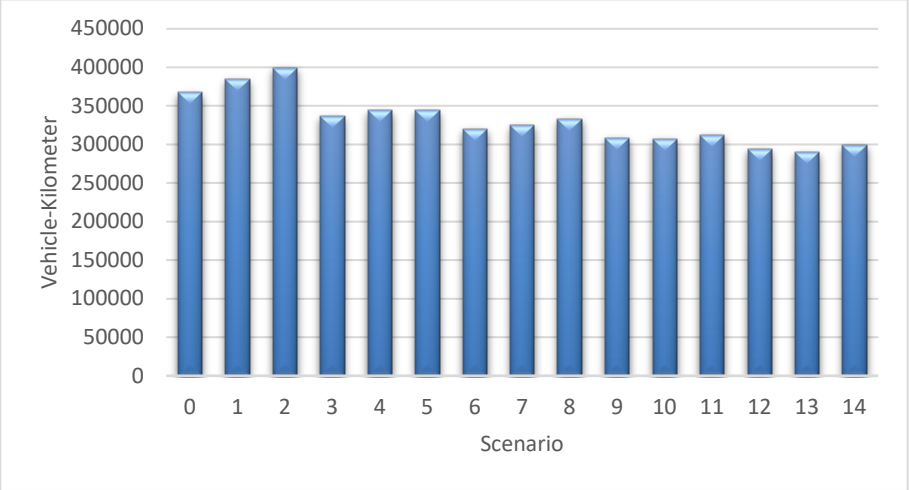

Figure 6.7 Total vehicle-kilometers traveled

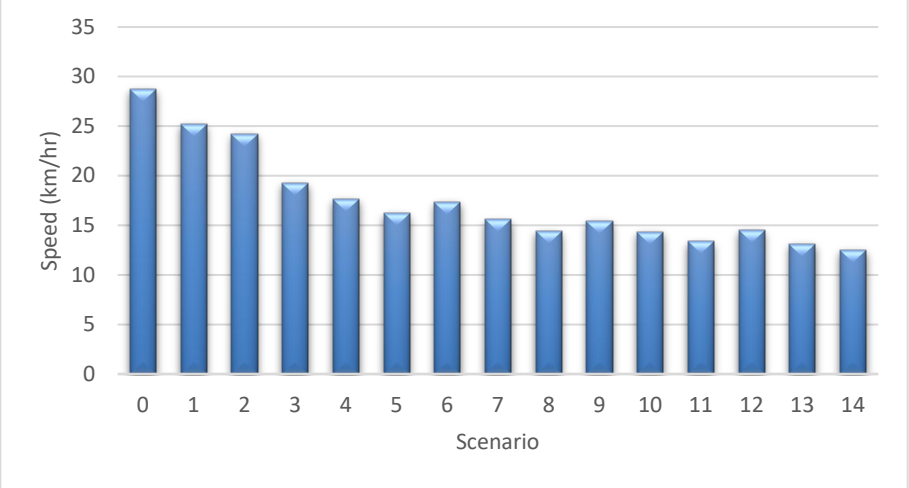

Figure 6.8 Average network speed

The network indicator evaluation clearly explains that when demand increases the trends in all scenarios increase as the number of vehicles entering the network increases. Indicators like travel time, waiting time, delay and VHT increase as flood depth increases. As the flood depth increases, congestion in the network increases. Vehicles are waiting a long time in congested traffic, while other vehicles are choosing alternative routes to reach the desired destination. Delays are increasing, as shown in Figure 6.6, with waiting time and traveling time also increasing, as shown in Figure 6.4. Due to the delays, traveling time and waiting time increase the vehicle-hours traveled and average speed increases and decreases accordingly, as shown in Figures 6.5 and 6.8. Vehicle-kilometers traveled in the network decreases as the flood depth increases, as shown in Figure 6.7 because the number of vehicles entering and exiting from the network decreases.

Elasticity values of the scenarios are shown in Tables 6.3 and 6.4. Table 6.4 shows the elasticity of the demand and flood depth increase condition. The elasticity of VKT and VHT was higher in the base scenario when compared with increasing flood depth scenarios. Therefore, floods highly impacted traffic behavior.

Table 6.3 Change rate of VHT and VKT

Scenario	Depth (cm)	Demand	VHT (veh-hr)		VKT (veh-km)	
			value	%change	value	%change
Baseline	Dry	+0%	13,059	0	367,119	0
1	Dry	+10%	15,566	19	384,243	5
2	Dry	+20%	16,857	29	399,508	9
3	(0-5]	+0%	17,927	37	336,990	-8
4	(0-5]	+10%	20,022	53	343,848	-6
5	(0-5]	+20%	21,941	68	343,890	-6
6	(5-10]	+0%	18,792	44	319,977	-13
7	(5-10]	+10%	21,536	65	324,519	-12
8	(5-10]	+20%	23,796	82	332,647	-9
9	(10-20]	+0%	20,567	57	308,078	-16
10	(10-20]	+10%	22,012	69	307,355	-16
11	(10-20]	+20%	23,927	83	311,912	-15
12	(20-30]	+0%	20,933	60	294,442	-20
13	(20-30]	+10%	22,861	75	290,081	-21
14	(20-30]	+20%	24,541	88	298,855	-19

Table 6.4 Elasticity Analysis Using VHT and VKT

Depth (cm)	Demand	VHT (veh-hr)			VKT (veh.km)		
		value	%change	Elasticity	value	%change	Elasticity
Dry	10%	15,566	19	1.90	384,243	5	0.50
	20%	16,857	29	1.45	399,508	9	0.45
(0-5]	10%	20,022	53	5.30	343,848	-6	-0.60
	20%	21,941	68	3.40	343,890	-6	-0.30
(5-10]	10%	21,536	65	6.50	324,519	-12	-1.20
	20%	23,796	82	4.10	332,647	-9	-0.45
(10-20]	10%	22,012	69	6.90	307,355	-16	-1.60
	20%	23,927	83	4.15	311,912	-15	-0.75
(20-30]	10%	22,861	75	7.50	290,081	-21	-2.10
	20%	24,541	88	4.40	298,855	-19	-0.95

REFERENCES

1. Gliebe, J. and Å. Bergman, Case Study Evaluation of Dynamic Traffic Assignment Tools. 2011.

CHAPTER 7

TRAFFIC MANAGEMENT DURING FLOOD

In this chapter, scenario 12 (the baseline scenario where the highest flood is 20-30 centimeters) with and without traffic management measures are simulated in the model. Results are compared to investigate the improvement of road network performance after implementation of traffic management measures.

7.1 Optimization of signal

Traffic signal control is one of the traditional traffic management systems used in the world. There are many different types of traffic control systems including fixed time control, coordinated control-type, and actuated control-type. Traffic signal controllers function based on signal timing plans that contain phase configurations and parameters. In Bangkok, there are different types of traffic intersections with diverse types of traffic signal controls and disparate time plans. Thus, it becomes difficult to see the traffic signal timing plans for every intersection.

This study followed the optimization of signal control time plan produced by PTV Vissim using genetic algorithms. Genetic algorithm optimizations of traffic signal timings are based on the average delay at the intersection for all the movements. Average delay of all the vehicles that pass through the signal heads at the intersection can be automatically determined from the node evaluation in Vissim.

To optimize the signal stages, highest delay time in all the stages were determined Stages with minimum and maximum times were adopted as the best and worst stages. Worst stages green time was adjusted by deducting the time from the best stage. If the time could not be deducted from the best stage, the next best stage was selected to deduct. Similarly, the remaining stages were also optimized for signal timing. This optimized signal timing for traffic management is shown in Figure 7.1.

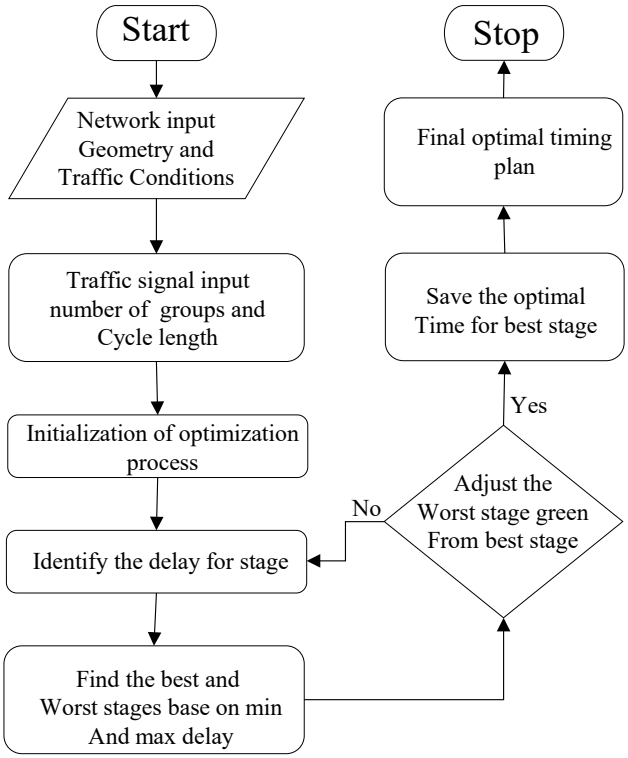

Figure 7.1 Signal optimization Framework

7.2 Use of the elevated Metropolitan expressway with free tolls

This concept of an Expressway with free tolls during flooding was suggested by Geroliminis and Levinson [1] as an application of the MFD congestion pricing strategy (generalized cost). The result can improve mobility and relieve congestion in cities by reducing delays and the length of the rush hour.

To apply in this measure are defined generalize cost in expressway for this scenario same another road type which provides a simplified description of travelers' choices the effect of flood scenarios in their decisions to improve the city's mobility. In this measure in a macroscopic model for both (travelers) demand and road network (supply) are critical situations as peak hour demand and road network where traffic can still operate. This scenario can describe the dynamic nature of policy decisions that will address the induced demand.

7.3 Traffic management during flooding

The simulation period to evaluate how vehicles entered and exited the network during floods covered only peak hours. The numbers of vehicles entering and exiting, as shown by the model, were consistent for all scenarios.

Table 7.1 Result of traffic management measures

Performance Criteria	Scenario 12	Traffic management measures					
		Free toll		Optimized signal		Free Toll & Optimized signal	
		value	Change%	value	Change%	value	Change%
In Count(veh)	65,275	68,862	+5.50	76,380	+17.01	81,333	+24.60
Out Count (veh)	53,433	56,755	+6.22	65,612	+22.79	73,768	+38.06
Waiting(veh)	139,694	133,686	-4.30	91,242	-34.68	82,559	-40.90
Travelling(veh)	100,768	95,303	-5.42	85,720	-14.93	70,756	-29.78
VHT(veh-hr)	20,934	19,538	-6.67	17,719	-15.36	15,209	-27.35
VHD(veh-hr)	15,430	13,596	-11.89	12,414	-19.55	9,512	-38.35
VKT(veh-km)	294,442	335,757	+14.03	343,741	+16.74	383,872	+30.37
Density(veh/km)	23	22	-6.67	20	-15.35	17	-27.35
Speed(km/hr.)	14	18	+21.55	20	+38.10	26	+77.65

Results in Table 7.1 show that traffic management measures during flooding improved the effectiveness of scenario 12 (Increased demand 20% and flood depth 20-30 cm). Using the elevated Metropolitan expressway with free tolls showed a slight increase in the number of vehicles entering and exiting the road network, thus slightly improving the VHT as vehicles chose alternative routes for traveling. By optimizing the signals, the number of vehicles exiting the network increased by 22% and improved VHT by a 15% reduction. Overall, optimization of the signal condition showed better results than the use of the elevated Metropolitan expressway with free tolls in scenario 12. Signal optimization impacted the overall network, whereas use of the elevated Metropolitan expressway with free tolls applied only on limited roads (expressway).

When use of the elevated Metropolitan expressway with free tolls and optimization of the signal network were applied together, the number of vehicles exiting the network or completing trips increased by 38%, VHT decreased by 27%, and VKT increased by 30%. Overall, a substantial improvement in the network was realized.

In summary, results showed that VHT after applying traffic management measures by all vehicles reflected an overall performance of the whole network. Network VHT reduced with higher out count and reduced delays (VHD). The decrease of VHT indicated a better traffic situation, with average speed increased, while delays either in the network or of an individual vehicle declined. Another criterion is VKT by vehicles. Like VHT, VKT is meaningless to reflect the change of traffic demand in this case. Nevertheless, when combining with VHT, VKT indicates the extent that drivers change their route choices and this affects network performance. Sometimes, other criteria such as average speed and delay are also considered. However, evaluation results are mostly represented by travel time and travel distance.

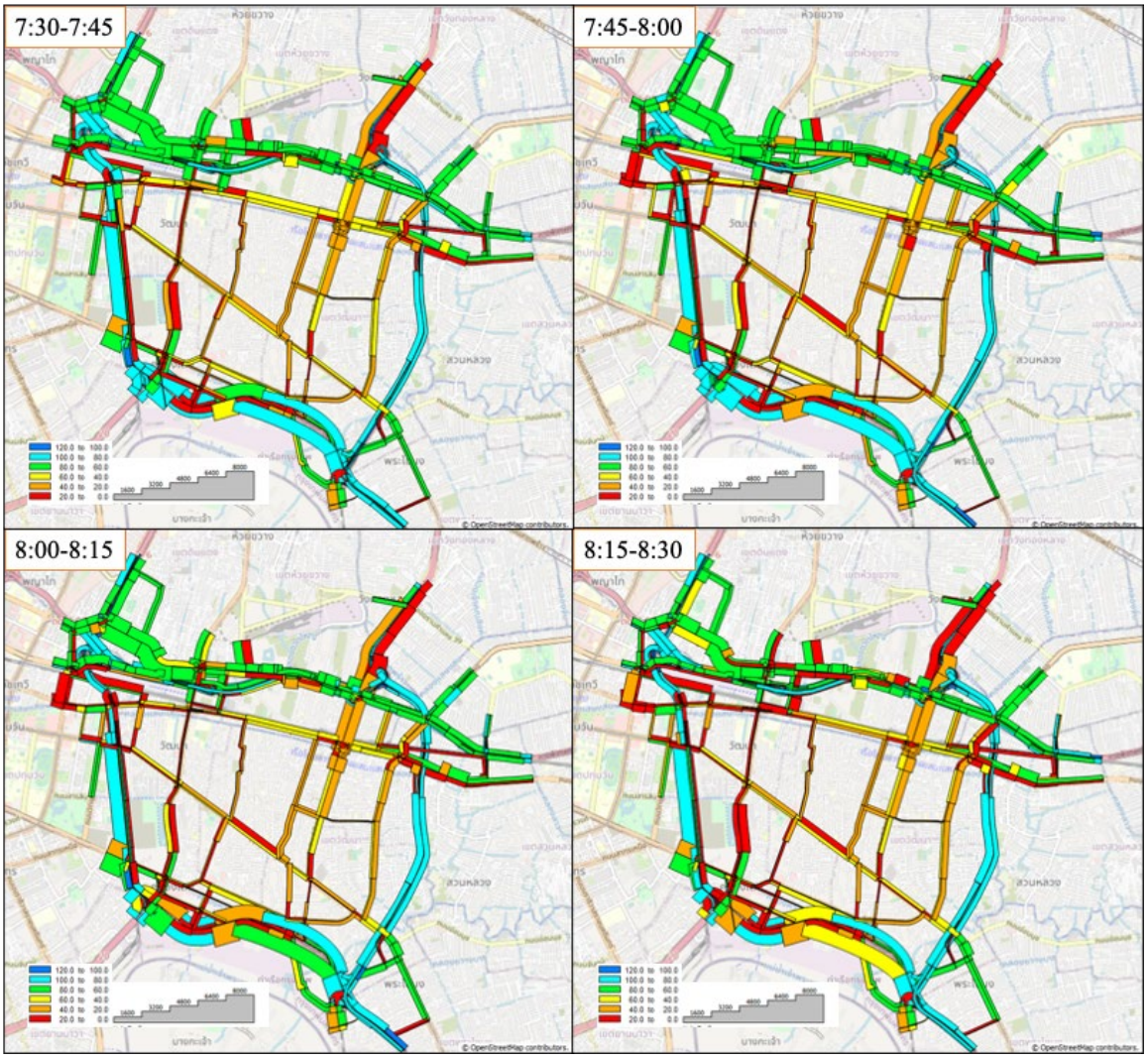

Figure 7.2 Speed and flow after expressway with free tolls measure

Figure 7.2 shows the speed and flow distribution in the network at 15-minute intervals during the morning peak (from 7:30 to 8:30 am) for the scenario 12 with expressway with free tolls measure. The thickness of the link indicates flow, while color represents speed. Narrow or reduced thickness links contain flow of 1600 veh/hr, with increasing trend in the thickness giving flows of 3200, 4800, 6400, and 8000 veh/hr, respectively. Similarly for speed, red color represents the lowest speed of 0 to 20 km/hr and blue color represents the highest speed of 100 to 120 km/hr. The first 15-minutes has the highest flow and highest speed but the trend decreases gradually during the subsequent 15-minute intervals. Speed should increase with decrease in flow but here the speed also decreases because of congestion levels.

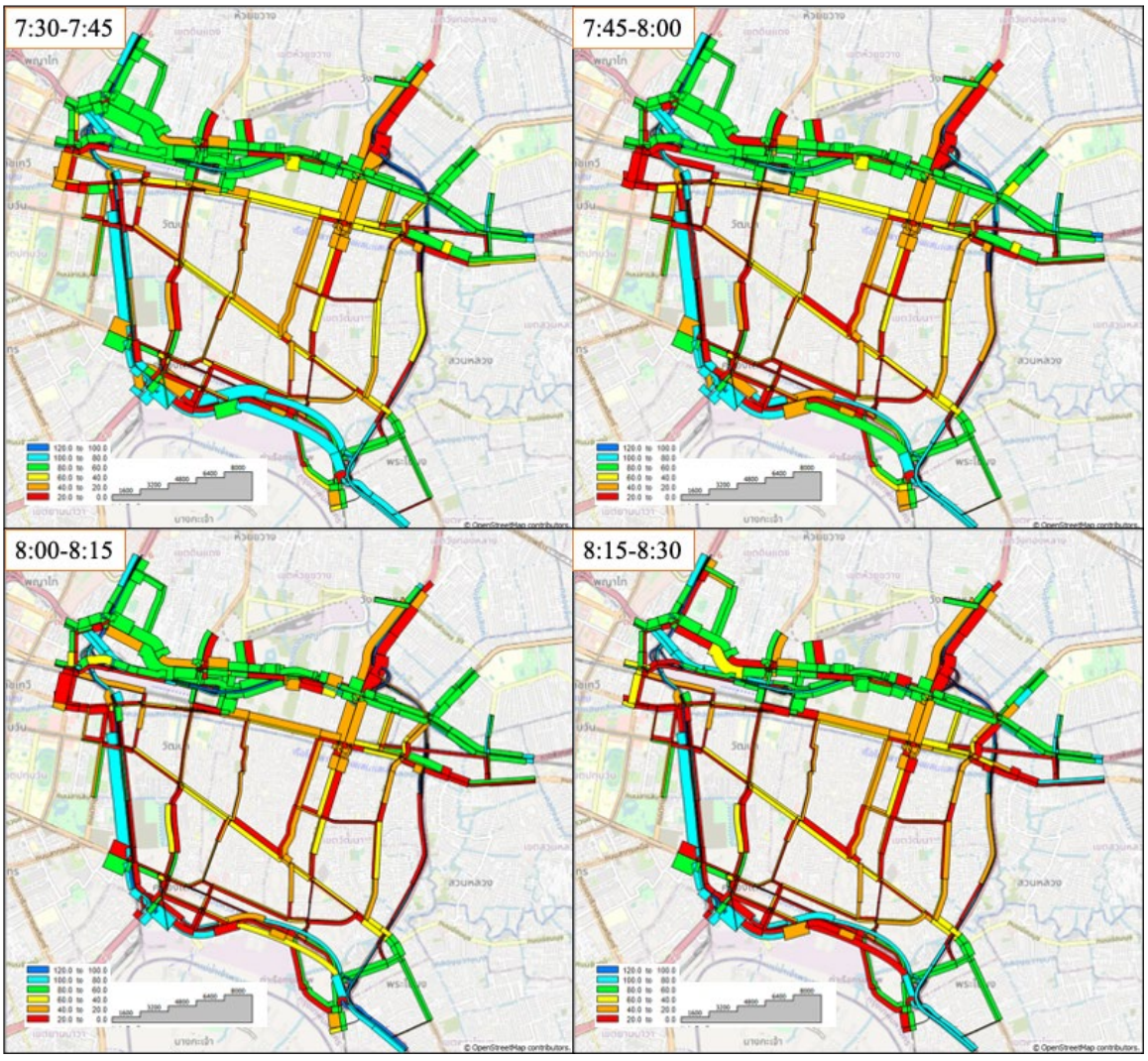

Figure 7.3 Speed and flow after optimization of signal measure

Figure 7.3 shows the speed and flow distribution in the network at 15-minute intervals during the morning peak (from 7:30 to 8:30 am) for the 12th scenario with optimization of signal measure. The thickness of the link indicates flow, while color represents speed. Narrow or reduced thickness links contain flow of 1600 veh/hr, with increasing trend in the thickness giving flows of 3200, 4800, 6400, and 8000 veh/hr, respectively. Similarly for speed, red color represents the lowest speed of 0 to 20 km/hr and blue color represents the highest speed of 100 to 120 km/hr. Inner links of the network have almost the same flow and speed for all time intervals but outer links in the network change. The first 15-minutes has the highest flow and lowest speed, while for subsequent 15-minute intervals flow decreases gradually but speed increases on links with high flow and decreases on links with less flow. This occurs because signal optimization is done based on the flow. Links with high flow will give highest green time, while links with less flow will be given less green time.

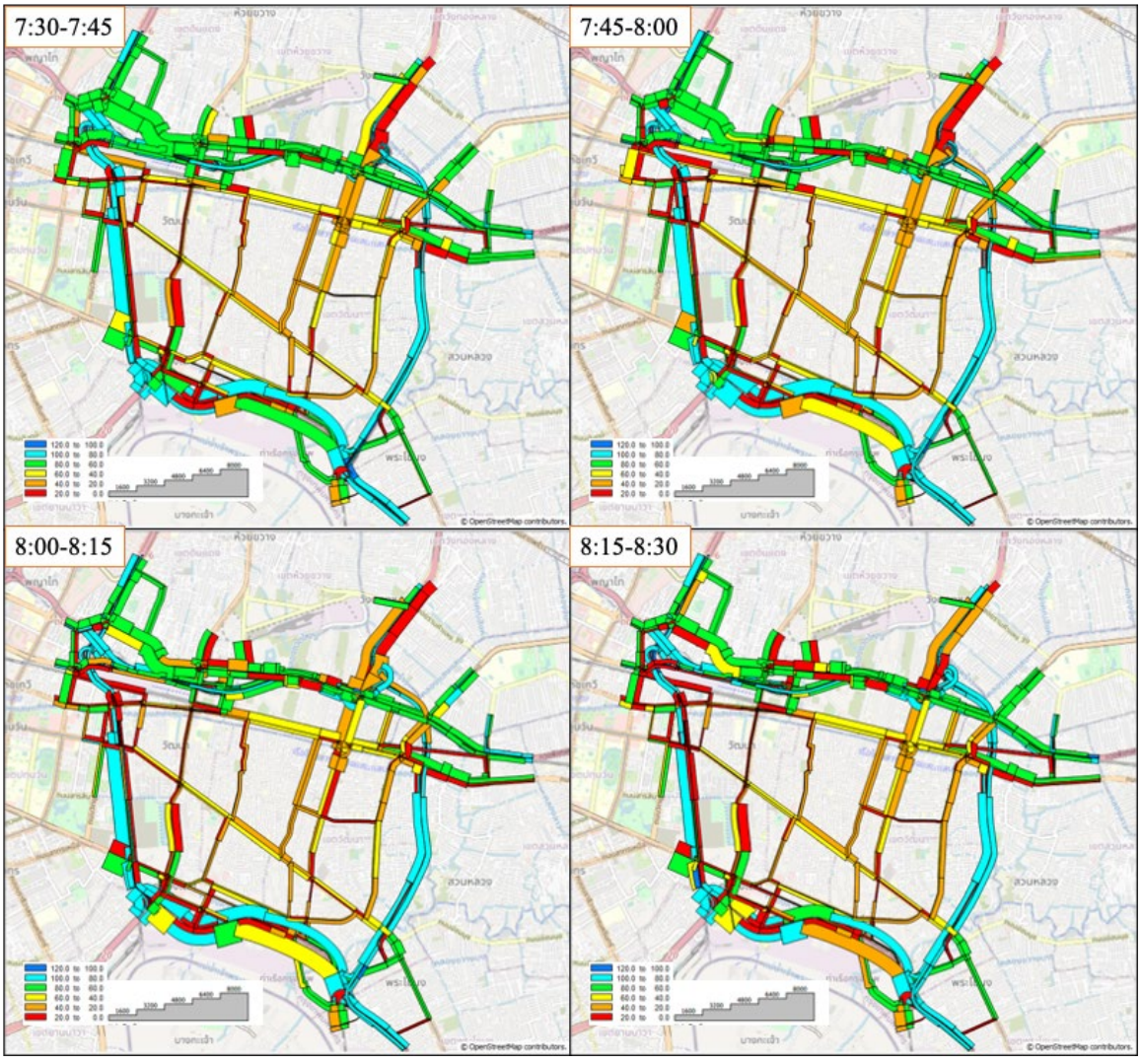

Figure 7.4 Speed and flow after combining expressway with free tolls and optimized traffic signal measures

Figure 7.4 shows the speed and flow distribution in the network at 15-minute intervals during the morning peak (from 7:30 to 8:30 am) for the 12th scenario with both expressway with free toll and optimization of signal measures. The thickness of the link indicates flow, while color represents speed. Narrow or reduced thickness links contain flow of 1600 veh/hr, with increasing trend in the thickness giving flows of 3200, 4800, 6400, and 8000 veh/hr, respectively. Similarly for speed, red color represents the lowest speed of 0 to 20 km/hr and blue color represents the highest speed of 100 to 120 km/hr. Inner links of the network have almost the same flow and speed for all time intervals but outer links in the network change. The first 15-minutes has the highest flow and highest speed, while for subsequent 15-minute intervals the trend decreases gradually because of congestion levels.

REFERENCES

1. Geroliminis, N. and D.M. Levinson, Cordon pricing consistent with the physics of overcrowding, in Transportation and Traffic Theory 2009: Golden Jubilee. 2009, Springer. p. 219-240.

CHAPTER 8

CONCLUSIONS

8.1 Conclusions

MFD captures the relationships between these characteristics and plays an essential role in traffic flow theory and transportation engineering. MFD derived from detector data of signalized sections is greatly affected by the location of the detectors [1] and the use of vehicle trajectories using probe vehicles has been encouraged in the literature [2]. The literature review determined that the MFD shape changed as a result of network traffic operation under different flood levels. Varying degrees of impact induce MFD shape change, and scatter occurs compared with dry conditions. Flood levels have different degrees of impact on the stability and certainty of the road network. At less than 5 cm flood depth the MFD shape only slightly changed, with a clear difference in MFD shape change when flood levels increased from 5 cm to 20 cm. Flood levels exceeding 30 cm had greater effects on the discreteness of the MFD. The equation presenting the relationships between macroscopic traffic variables such as density, flow, and speed under different flooding depths indicated the R-square value reduced as flood depth increased, while continuity decreased. When assessing the MFD key parameters, an increase in flood conditions caused a reduction in free-flow speed at -8.3%, -19.4%, -27.7%, and -30.5% respectively, while maximum flow of the network reduced by 30.5%, 49.6%, -28.3%, -38.1%, -42.1% and-49.6%, respectively with density slightly reduced.

Models that predict short-term traffic flow using historical and real-time data are useful to assess current impacts on transportation systems and determine the implementation of a specific strategy. Dynamic traffic assignment (DTA) is a well-balanced approach between large scale with a low level of detail in macro models, and small scale with high fidelity in micro models. By implementing dynamic user equilibrium and the time-dependent nature of demand and network characteristics, a DTA model produces more realistic traffic conditions at a large scale with reasonable effort for data preparation, network coding, and calibration. This study used a mesoscopic model because this was able to simulate the movements of individual vehicles along roadway links using macroscopic traffic flow relations (free-flow speed, maximum flow, and jam density). We defined these values according to the remaining efficiency of the road network at each flood condition. Our results offer a novel view of dynamic traffic conditions and provide rational scenario comparisons that are only possible with an equilibrium-based solution.

This analysis of the impact of floods on traffic conditions used a calibrated mesoscopic traffic model as a baseline and introduced 14 test alternatives. 1) Model convergence showed that flood depth increased relative gap patterns were very similar, while convergence curves matched each other well. In terms of network convergence, when demand increased, the model generated more fluctuations and the relative gap increased, indicating that the network was more congested. Traffic between an OD pair switched back and forth among a few alternative routes. The model was more sensitive to demand change than MFD parameter changes. 2) Tests on network indicators and elasticity analysis on VKT and VHT were conducted to investigate the impacts of perturbations of input parameters over the simulation results. Vehicle kilometers traveled decreased in the network as the flood depth increased because the number of vehicles entering and exiting from the network decreased. The elasticity of VKT and VHT was higher in the base scenario when compared with increasing, flood depth scenarios; thus, floods had a high impact on traffic behavior. The model showed reasonable capability to accommodate some network uncertainty without risking overall credibility. The base year model was more sensitive to change in demand than the MFD. Two traffic management measures were selected to analyze their effects on network performance. In scenario 12, as the present critical scenario, results indicated that road network performance of the whole network improved. Optimizing the signal control system improved network performance more than Expressway with free tolls by 7% in VHT and more than 2% in VKT. However, combining the two measures for traffic management improved network performance by more than 27% in VHT and 30% in VKT compared to the critical scenario.

8.2 Recommendations

Subarea extraction causes loss of the temporal dimension of demand. The current process of extracting subarea demand from a regional model results in a loss of the temporal dimension of that demand and should be improved. Subarea extraction is necessary to generate trip tables for DTA because eBUM is applied for the whole country, whereas this study concerned only the Sukhumvit area. The proposed approach maintained the external traffic analysis zone (TAZ) for trips ending outside the Sukhumvit area, allowing the time-of-day demand to be tabulated directly from the trip lists. This could be important if, for example, the work trips departing from the CBD tended to all leave at the same time, causing a specific surge of traffic in part of the network.

This study considered MFD shape comparisons for a single reservoir. Future investigations should examine flow exchanges in multi-reservoirs to assess the principle of MFD-based modeling over multiple regions (Figure 8.1).

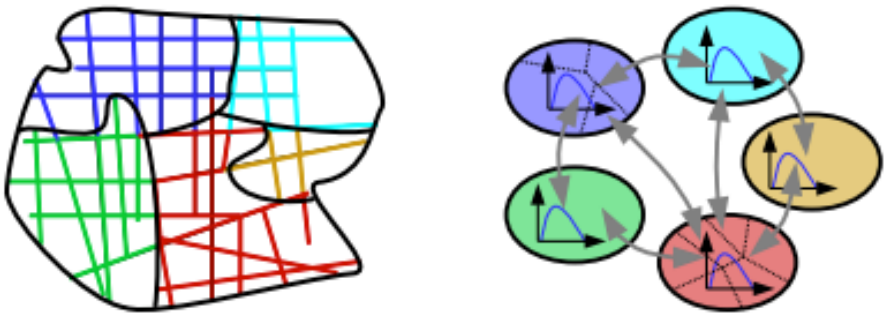

Figure 8.1 Partitioning in different urban regions.

Figure 8.1. shows a simple formulation of traffic dynamics within a region, together with a limited number of calibration parameters to develop efficient control schemes. The main idea is to protect a given area by limiting inflow at its periphery to maintain maximum throughput. In practice, inflow limitation can be achieved by tuning traffic light timings or road pricing.

REFERENCES

1. Courbon, T. and L. Leclercq, Cross-comparison of macroscopic fundamental diagram estimation methods. *Procedia-Social and Behavioral Sciences*, 2011. 20: p. 417-426.

2. Leclercq, L., N. Chiabaut, and B. Trinquier, Macroscopic fundamental diagrams: A cross-comparison of estimation methods. *Transportation Research Part B: Methodological,* 2014. Vol.62, p.1-12.